Atmos. Meas. Tech. Discuss., 5, 1153–1231, 2012
www.atmos-meas-tech-discuss.net/5/1153/2012/
doi:10.5194/amtd-5-1153-2012

Atmospheric Measurement Techniques Discussions

Development of parallel sampling and analysis for the elucidation of gas/particle partitioning of oxygenated semi-volatile organics: a limonene ozonolysis study

S. Rossignol[1,2], L. Chiappini[1], E. Perraudin[2,*], C. Rio[1], S. Fable[1], R. Valorso[2], and J. F. Doussin[2]

[1]Institut National de l'Environnement Industriel et des Risques, Parc Technologique ALATA, 60550 Verneuil-en-Halatte, France
[2]LISA, Universités Paris-Est-Créteil et Paris Diderot, CNRS – UMR7583, 61 Av. du Général de Gaulle, 94010 Créteil, France
[*]now at: EPOC, University of Bordeaux, CNRS – UMR5805, 351 Cours de la Libération, 33400 Talence, France

Received: 9 January 2012 – Accepted: 23 January 2012 – Published: 6 February 2012

Correspondence to: L. Chiappini (laura.chiappini@ineris.fr)

Published by Copernicus Publications on behalf of the European Geosciences Union.

Abstract

Gas/particle partitioning behaviour of secondary organic matter semi-volatile fraction and the associated multiphase chemistry are key features to accurately evaluate secondary organic aerosol climate and health impacts. However, today, oxygenated secondary species partitioning is rarely assessed in experimental SOA studies and SOA modelling is still largely based on estimated partitioning data. This paper describes a new analytical approach, solvent free and easy to use, to explore the chemical composition of the secondary organic matter at a molecular scale in both gas and particulate phases. The method is based on thermal-desorption (TD) of gas and particulate samples, coupled with gas chromatography (GC) and mass spectrometry (MS), with on sampling supports derivatisation processes. Gaseous compounds are trapped on PFBHA or MTBSTFA pre-coated Tenax TA adsorbent tubes. Particulate samples are collected onto quartz or Teflon-quartz filters and subsequently exposed to PFBHA or MTBSTFA derivatisation reagents before TD-GC-MS analysis. Method development and validation are presented from an atmospherically relevant range of organic acids and carbonyl and hydroxyl compounds. Method application to a limonene ozonolysis experiment conducted in the EUPHORE simulation chamber under close-to-real conditions of low concentrations and relative humidity provides an overview of the method abilities. 25 compounds have been positively or tentatively identified, 9 being in both gaseous and particulate phases and 11, among them tri carboxylic acids, hydroxyl dicarboxylic acids and oxodicarboxylic acids, being detected for the first time.

1 Introduction

Atmospheric formation of particulate matter from organics gas-to-particle transfer during their atmospheric oxidation is now considered as one of the main phenomena involved in both air quality and climate issue (IPCC, 2007; Hallquist et al., 2009). Better understanding of the interrelated processes and better representation in models is still

AMTD
5, 1153–1231, 2012

required (Kanakidou et al., 2005). Secondary Organic Aerosol (SOA) formation is commonly described by gas to particle conversion of semi and non-volatile secondary species formed in the gas phase by atmospheric oxidation of Volatile Organic Compounds (VOCs) precursors (e.g. Seinfeld and Pankow, 2003; Asher and Pankow, 2006; Odum et al., 1996). However, for SOA formation and evolution pathways, in addition to the initial gas phase oxidation processes, a significant number of studies of the last decade has pointed out the role of multiphase chemical processes, in the particle phase (e.g. Graber and Rudich, 2006; Kroll et al., 2007; Healy et al., 2008; Monks et al., 2009) or at the gas–particle interface (e.g. Rudich, 2003; Rudich et al., 2007). These processes involve continuous modification of SOA chemical composition and physicochemical properties and interdependently influence the partitioning of semi-volatile organic species (SVOCs) between gaseous and aerosol phases, consuming or forming SVOCs (Healy et al., 2008).

Hence, multiphase chemical processes' understanding is today a key feature to assess both aerosol climate impacts and health effects. It can improve climate impact evaluation through modelling enhancement of formation and evolution pathways and aerosol physical properties characterisation. In term of health issue, knowledge of SOA formation pathways and fine composition in different outdoor/indoor conditions is required for toxicological evaluation.

In spite of large progress in recent years (e.g. Donahue et al., 2006; Camredon et al., 2010; Parikh et al., 2011), current SOA formation and evolution modelling, often suffers from discrepancies between modelling results and observations (e.g. Volkamer et al., 2007; Chan et al., 2009; Pankow, 2011) that notably reveals lacks in our knowledge of SOA formation and aging pathways. Atmospheric chemistry models integrating SOA formation are usually based on the parameterisation of $SVOC_i$ gas-particle partitioning proposed by Pankow (2006). This parameterization is based on the definition of an equilibrium partitioning coefficient $K_{p,i}$ ($m^3\ \mu g^{-1}$):

AMTD
5, 1153–1231, 2012

$$K_{p,i} = \frac{\left(\text{ng}\ \mu\text{g}^{-1}\right)_{\text{particle phase}}}{\left(\text{ng}\ \text{m}^{-3}\right)_{\text{gas phase}}} = \frac{P_i}{G_i\ M} \quad (1)$$

where P_i is the mass concentration (ng m^{-3} air) of the SVOC$_i$ in the particle phase, G_i is the mass concentration (ng m^{-3} air) of the SVOC$_i$ in the gas phase and M is the mass concentration (µg m^{-3} air) of the total sorbing particle phase. While Eq. (1) is sorption process nature independent – i.e. adsorption or absorption (Lazaridis, 1999) – most of the models assumes an absorptive gas/liquid partitioning of SVOCs as this mechanism is expected to be predominant in SOA formation (Pankow, 1994; Odum et al., 1996) and links $K_{p,i}$ with the saturation vapour pressure of the SVOC$_i$ trough the Eq. (2):

$$K_{p,i} = \frac{760\ R\ T}{10^6\ \overline{\text{MW}_{\text{om}}}\ \gamma_i\ P^{\text{o}}_{\text{L},i}} \quad (2)$$

where R (m^3 atm mol^{-1} K^{-1}) is the ideal gas constant, T (K) is temperature, $\overline{\text{MW}_{\text{om}}}$ (g mol^{-1}) is the mean molecular weight of the absorbing particulate material, γ_i is the activity coefficient of compound i in the particulate phase, and $P^{\text{o}}_{\text{L},i}$ (Torr) is the vapour pressure of compound i as a pure liquid (subcooled, if necessary).

SOA modelling based on chemical oxidation scheme (e.g. Jenkin, 2004; Camredon et al., 2007; Bessagnet et al., 2008; Chan et al., 2009; Valorso et al., 2011) generally estimate theoretical $P^{\text{o}}_{\text{L},i}$ using group contribution methods (e.g. Arp and Goss, 2009; Barley and McFiggans, 2010) and usually sets γ_i to unity, due to experimental determination difficulties. This can lead to uncertainties suspected to account for observed discrepancies between models and real atmosphere observations in SOA yields. Another likely major source of discrepancies could be the poor consideration of multiphase chemical processes as a sink or a source of SVOCs (Chan et al., 2009). An alternative modelling approach to the mechanistic description of SOA is the Volatility

AMTD
5, 1153–1231, 2012

Basis Set (Donahue et al., 2006, 2009; Farina et al., 2010; Tsimpidi et al., 2010; Cappa and Jimenez, 2010) which is based on distribution of considered organic matter mass into volatility classes according to saturation mass concentration C_i^* (corresponding to the inverse of the Pankow type partitioning coefficient). In this case, dilution process and evolution of particulate mass are the driving features. While VBS scheme does not directly integrate chemical mechanisms, it takes reactivity into account considering a redistribution of the organic mass from one volatility bin to another. VBS consequently requires data to link atmospheric relevant partitioning behaviour to organic aerosol origin and composition. This context highlights requirement in enhancing our comprehension of multiphase chemical mechanisms, especially those driving SVOCs formation and consumption, and providing atmospheric relevant data on SVOCs partitioning behaviour. There is therefore a strong necessity to simultaneously explore the molecular composition of both gas and particulate phases in SOA studies, and to systematically determine the observed SVOCs partitioning. The related experimental data have to be evaluated not only with low concentration simulation chamber experiments but also using real atmospheres to assess the relevance of simulated atmospheres results.

However, since it results from complex and successive oxidation processes, the atmospheric secondary organic matter is highly functionalized and reactive. It contains oxygenated moieties such as aldehydes, ketones, alcohols, carboxylic acids, etc. Exploring SOA chemical composition and the associated gas phase at molecular scale is consequently a true analytical challenge (Prather et al., 2008). This is emphasized when the atmospheric relevant constraints of low concentration levels and relative humidity are taken into account.

Until today, only a few studies have been assessed the partitioning of secondary organic compounds through determination of partitioning coefficients K_p for individual secondary species. Some papers report the use of a thermodenuder (de Gouw and Warneke, 2007; Grieshop et al., 2009; Lee et al., 2011) in order to evaluate volatility of SOA formed from different precursors without chemical composition information. In

AMTD
5, 1153–1231, 2012

these studies, SOA formed in simulated atmospheres flows and evaporates through a temperature controlled tube, previously calibrated with known vapour pressure compounds. By this method SOA mass is divided into volatility classes with known vapour pressure ranges, providing a volatility distribution of SOA mass. This method is very useful to provide atmospheric relevant constraints for modelling based on the Volatility Basis Set (Grieshop et al., 2009) and evaluate the semi-volatile and non-volatile fractions of SOA. Nevertheless, it remains incomplete as it provides no insight into chemical processes.

Studies aiming at elucidating chemical processes focus on the characterisation of secondary organic matter chemical composition at a molecular scale. However, while the aerosol phase is most often analysed by chromatographic off-line methods in order to explore its highly complex molecular composition, the gas phase products are most often monitored by on-line method providing less insights into molecular composition. Today, Proton Transfer Reaction - Mass Spectrometry (PTR-MS) is the most employed on-line technique for the gas phase composition elucidation (e.g. Blake et al., 2004; Kroll et al., 2006) as it provides continuous structural information and quantification of gas phase compounds at very low concentration levels, around 10 ppt, especially for small molecules (Warscheid et al., 2003) without water interferences. It thus can be used in real atmosphere. Nevertheless, PTR-MS is not specific.

Chromatographic methods using on- or off-line approach, often coupled with thermal-desorption, are sometimes applied to elucidate gas phase molecular composition. However, apart from a few approaches using derivatisation process (e.g. Ho and Yu, 2002, 2004; Temime et al., 2007; Pacolay et al., 2008), these techniques are limited to non polar or mono-functionalized compounds (e.g. Wedel et al., 1998; Xu et al., 2003; Sinha et al., 2010) with limited interest for secondary chemistry studies.

Aerosol phase chemical composition focuses interest on studies aiming at secondary organic chemical mechanisms elucidation. To that purpose, a wider range of powerful analytical methods exists, mainly because of aerosol chemical complexity and diversity, divided between on-line and off-line methods (Hallquist et al., 2009). Over the past

AMTD
5, 1153–1231, 2012

decade, on-line real-time Aerosol Mass Spectrometry (AMS) has become a technique of choice to explore the aerosol phase chemical composition with high time resolution (Sullivan and Prather, 2005; Canagaratna et al., 2007). Combining direct thermal extraction of sampled airborne aerosol (flash vaporisation upon impaction on a hot surface, ~600 °C, under high vacuum) with Electronic Impact (EI) ionisation and mass spectrometry, AMS provides data on particulate organic matter nature – sulphate, nitrate, ammonium and chloride contents and oxidation state with function types identification (alcohols, carboxylic acids, carbonyls) – and is consequently a powerful tool to chemically and physically characterize SOA. It was successfully applied to both real (e.g. Zhang et al., 2011) and simulated atmospheres (e.g. Sato et al., 2010). However, complex mass spectra resulting from total particle extensive EI fragmentation does not allow unambiguous identification of individual organic compounds, which limits composition exploration at a molecular scale.

Another in-situ interesting method is the TAG instrument, coupling Thermal desorption Aerosol with Gas chromatography and Mass Spectrometry (MS) detection/Flame Ionisation Detector (FID) (Williams et al., 2006). Recently improved by GCxGC separation (2D-TAG, Goldstein et al., 2008; Isaacman et al., 2011), TAG provides detailed data on particle components volatility distribution with a good time resolution (from 1 to 2 h). However gas chromatographic separation limits TAG detection and identification range to non polar and mono-functionalized compounds and then does not allow insight into SOA chemistry.

Off-line chromatographic methods are required to access the high complexity of SOA composition. They differ in first instance by the extraction step. Hays and Lavrich (2007) proposed an interesting review on Thermal Desorption coupled with Gas Chromatography and Mass Spectrometry (TD-GC-MS) applied to fine aerosol, which has the main advantages to be fully automated, inexpensive, sensitive and solvent-free. However, like on-line TAG, these techniques are limited by SOA compounds polarity. To overcome this limitation, introduction of an in-situ derivatisation step can be performed. A few recent studies have integrated this principle, exposing

AMTD
5, 1153–1231, 2012

sample filters to derivatisation reagent for methylation or trimethylsilylation during thermal desorption for the detection and quantification of mono- and di-carboxylic acids (Beiner et al., 2009; Sheesley et al., 2010; Orasche et al., 2011). Other extraction techniques, more scarcely used, can be reported. As an example, Supercritical Fluid Extraction (SFE) couples the extraction step directly to the analytical process. Its efficiency for extracting organic compound from complex matrices was demonstrated coupling SFE with GC-MS or Liquid Chromatography-GC-MS (LC-GC-MS) (Hansen et al., 1995; Forstner et al., 1997; Castells et al., 2003). The process has the advantages to allow derivatisation of polar compounds during the static extraction step (Shimmo et al., 2004; Chiappini et al., 2006). Nevertheless, the large majority of studies exploring organic aerosol fine chemical composition is based on a first solvent sample extraction step as it provides a huge range of possibilities for further analytical processes. Solvent extraction type and steps to be considered (solvents choice, ultrasonication, Soxhlet, pre-concentrations steps, derivatisation, etc.) are selected according to both the fraction of organic mass studied (water soluble organic compounds, PAHs, carbonyl, carboxyl and/or hydroxyl compounds, organosulphates, organonitrates, oligomers, humic-like substances, etc.) and the analytical technique employed (GC, LC, Ion Chromatography – IC, electrophoresis, etc.). Mass spectrometry detection is largely used for identification and quantification. Among the various possible combinations, those aiming at polar and functionalized compounds analysis (carbonyl, carboxyl and hydroxyl groups containing molecules) are mainly divided between derivatisation/ GC-MS analysis (e.g. Nolte et al., 2001; Claeys et al., 2004, 2007; Edney et al., 2005; Szmigielski et al., 2007; Chan et al.,2010; Vivanco et al., 2011) and direct LC-soft ionization-MS analysis (electrospray ionisation, ESI-MS or atmospheric pressure chemical ionisation APCI-MS) (Kitanovski et al., 2011). These techniques are constantly improved and made more complex in order to gain on detection limits, enlarge the separable species range (GC × GC, LC × LC), or increase our identification ability through additional spectral data or high resolution MS (e.g. MS^n, ion trap – ITMS, Time of Flight – ToFMS, Fourier Transform Ion Cyclotron Resonance Mass Spectrometry – FTICR-MS)

AMTD
5, 1153–1231, 2012

(e.g. Hamilton et al., 2005; Pol et al., 2006; Claeys et al., 2009; Yasmeen et al., 2011; Hamilton et al., 2011). Nevertheless, while solvent extraction has proven efficiency for subsequent quantification and precise molecular structure identification, related protocols are time-consuming, and are prone to contamination and losses, especially for the semi-volatile fraction, during the different extraction steps.

Global approaches considering gas and particulate phases simultaneously are required to elucidate secondary organic matter at a molecular scale for both phases and provide relevant SVOCs partitioning data. Most works aiming at studying SVOCs partitioning are based on off-line chromatographic techniques coupled to mass spectrometry, for both phases. This approach involves simultaneous sampling of both gas and particulate phases. One of the most common sampling methods is to trap gas phase compounds on one or more annular glass denuder (XAD-4 coated) placed in series with filter collecting the aerosol phase. This sampling technique is applied without any derivatisation step prior to gas GC – MS analysis in order to investigate gas/particle partitioning of non-polar compounds – alkanes, PAHs (Volckens and Leith, 2003), or small carbonyls in diesel exhaust (Lee et al., 2004; Jakober et al., 2008). In more specific SOA studies, consequently looking for poly-functionalized and reactive compounds (carbonyls, hydroxyls, carboxyls), a derivatisation step is introduced prior to chromatographic separation. After solvent extraction of both denuder and filter, each sample is derivatised, in liquid phase, by addition of a PFBHA solution. Extracts are then reduced and blown to dryness before reconstitution in an alternative solvent. Double derivatisation is then achieved by addition of a BSTFA solution and heating. Aliquots of the double derivatised extracts are injected in GC/MS (e.g. Woo and Kim, 1999; Kalberer et al., 2000; Jaoui et al., 2003). Alternative derivatisation reagents are sometimes employed, such as the BF3-methanol reagent (Jaoui and Kamens, 2003). In spite of a powerful capacity to identify and quantify individual species in complex mixtures of poly-functionalized compounds, this process still presents the disadvantages of solvent extraction. More recently, the same simultaneous sampling technique of both gas and particulate phases onto denuder/filter pack was improved for carbonyl measurements:

AMTD
5, 1153–1231, 2012

PFBHA is used prior to sampling to coat the XAD-4 denuder and impregnate the filter(s) (Temime et al., 2007; Healy et al., 2008, 2009; Ortiz et al., 2009). The sample treatment is thus reduced to a simple extraction of the sampling supports, denuders and filters, possibly followed by a reduction step and/or a filtering step. However, this method is reserved to carbonyls and solvent extraction is still required.

In this study we present a new analytical approach to explore, simultaneously, in parallel, the chemical composition of both gas and particulate phases and quantify the partitioning of individual and poly-functionalised SVOCs. Reducing both solvent use and time consuming sample treatment steps, this method is based on thermal-desorption (TD) of both gas and particulate phases sampling supports, coupled to gas chromatography (GC) and mass spectrometry (MS). It involves on-sorbent derivatisation of gas phase compounds and on-filter derivatisation of particulate phase compounds.

Method protocols validation is presented as well as their application in smog chamber experiment. Indeed, the method has been applied to two series of simulated atmosphere experiments performed in the EUPHORE European reactor. First series focuses on limonene ozonolysis chemical system while second series focuses on the isoprene photo-oxidation chemical system. Results from these experiments are used here to illustrate the method ability to explore secondary organic matter chemical composition in both gas and particulate phases.

2 Materials

2.1 Chemical

2.1.1 Standards

The standards used for the method development were chosen in order to fulfil the following purposes: (i) represent a wide range of functionalized semi-volatile secondary organic compounds and (ii) help the identification and quantification secondary

AMTD
5, 1153–1231, 2012

products expected from limonene ozonolysis (as this system has been chosen as a model system). Each series of compounds used for the different method characterisation tests is chosen in order to meet both experimental and objectives requirements. All chemicals were purchased from Sigma-Aldrich Co. (St. Louis, USA) with the exception of 4-oxopentanal synthesized by Diverchim SA (Montataire, France). Given the large compounds number used for both analytical development and limonene ozonolysis application, complete list is provided in the Supplement.

2.1.2 Derivatisation reagents

Derivatisation of oxygenated species blocks the reactive functions, reduces polarity and consequently enhances GC/MS response factors. Two derivatisation reagents were employed in order to derivatise either carbonyl compounds or carboxyl and hydroxyl compounds. O-(2,3,4,5,6-pentafluorobenzyl)hydroxylamine (PFBHA, purchase from Sigma-Aldrich: PFBHA hydrochloride, puriss. p.a., derivatisation grade for GC, ≥99.0 %) was used to derivatise carbonyl compounds (aldehydes, ketones). PFBHA derivatisation reaction (Fig. 1) forms oximes that provide characteristic fragmentation in MS and enhance detection limits. It is the most frequently used reagent in SOA studies to derivatise carbonyl groups (e.g. Wu and Hee, 1995; Jaoui et al., 2006; Carrasco et al., 2007; Healy et al., 2008; Ortiz et al., 2009). The reaction is commonly achieved in aqueous or water-containing solution (Cancilla and Que Hee, 1992). N-Methyl-N-(t-butyldimethylsilyl)trifluoroacetamide (MTBSTFA, purchase from Regis® Technologies Inc., MTBSTFA + 1 % *t*-BDMCS) was used to derivatise carboxyl and hydroxyl compounds. MTBSTFA reacts on labile hydrogen (Fig. 2) to form tertiobutyldimethylsilyl (TBDMS) esters with increased volatility compared to the parent compounds, and consequently extend the range of semi and non-volatile compounds observable in GC analysis. BSTFA is more largely employed in SOA studies than MTBSTFA (e.g. Kleindienst et al., 2004; Jaoui et al., 2006; Pietrogrande and Bacco, 2011), nevertheless

AMTD
5, 1153–1231, 2012

MTBSTFA was chosen since TBDMS derivatives provide similar fragmentation pathways with BSTFA derivatives but are less sensitive to hydrolysis.

2.1.3 Adsorbent

Gas phase sampling is achieved on adsorbent support. Tenax TA was chosen from three criteria (1) chemical inertia (2) capacity to trap compounds with a large range of volatility (3) highly hydrophobic nature. The commercial Tenax TA sorbent tubes were purchased from PerkinElmer, Inc. (Waltham, USA, stainless steel ATD Prepacked Sample Tubes, Sorbent: Tenax TA mesh 60/80). Before first use and after use, adsorbent tubes are conditioned overnight under heated helium flow (295 °C). Adsorbent cleanliness is checked before use by TD-GC-MS analysis.

2.1.4 Filters

Particulate phase sampling is achieved on two types of filters. To trap, PFBHA derivatise and analyse the carbonyl containing fraction of the aerosol phase, high-purity quartz microfiber filters (QM-A grade, 47 mm, Whatman™, Whatman International Ltd. Maidstone, UK) are used since quartz is the more thermal-resisting filter type commercially available. To trap, MTBSTFA derivatise and analyse the hydroxyl and carboxyl containing fraction of the aerosol phase, pure borosilicate glass fibres with fluorocarbon (tetrafluoroethylene, TFE) coating (Fiberfilm™, 47 mm, PallFlex®, Pall Life Sciences, Port Washington, USA) is used since TFE coating reduces reactivity of the filter surface and moisture loading during sampling. Thereafter, Fiberfilm™ filters are referred to as Teflon-quartz filters. Before use, quartz fibre filters are conditioned by heating at 450 °C for 5 h and Teflon-quartz filters by heating at 300 °C for 5 h.

To trap particles upstream the Tenax TA sorbent tubes, Teflon filter (Zefluor PTFE membrane filters, Pall Life Sciences, not analysed) are used.

AMTD
5, 1153–1231, 2012

2.2 Analytical systems

Two analytical systems were used to perform analytical development owing to a large samples number to be treated. A TD-GC-MS system was used for calibration curves achievement, detection limits evaluation and simulation chamber samples analysis. A TD-GC-FID was preferred for other method development tests as FID response stability over time facilitates avoids system calibration and facilitates results comparison. Both systems were used with the same analytical conditions. It goes without saying that only TD/GC/MS system is required to employ the developed method.

2.2.1 Thermal-desorption/gas chromatography/mass spectrometry system and procedures

The thermal desorption (TD) system is composed of (1) an Ultra 50:50 (Markes International, Llantrisant, UK) multi-tubes auto-sampler equipped with an injected sample split flow automated re-collection system, (2) an Unity 1 (Markes International) platform desorber for single tubes, (3) an Air Server (Markes International) used in mass flow controller mode. Samples are desorbed at 300 °C for 15 min at a flow rate of 50 ml min^{-1} and are cryogenically trap on-Tenax TA (mesh 60/80) adsorbent at −10 °C. The trap is desorbed for GC injection at 300 °C, for 15 min in order to clean the trap, with a split ratio of 1:9. Split flow from the injected sample is systematically re-collected, onto the same tube in the case of the gas phase samples, onto a cleaned Tenax TA tube in the case of the aerosol phase filter samples. The gas chromatography system is a 6890A from Agilent Technologies equipped with an Rxi®-5Sil MS column (60 m, 0,25 mm i.d., film thickness: 0.1 µm, Restek Corporation, Bellefonte, USA). Samples are chromatographically separated with the following temperature program: from 40 to 305 °C with a thermal ramp of 10 °C min^{-1}. The mass spectrometry system is a 5973 from Agilent Technologies. It is equipped either with an Electronic Impact source (EI at 70 eV), used in the case of the first injections of samples for structural identification and quantification, or a Chemical Ionisation source (CI in positive mode, methane as reagent gas),

AMTD
5, 1153–1231, 2012

used in the case of the injection of the re-collected samples to provide complementary structural information.

2.2.2 Thermal-desorption/gas chromatography/flame ionisation detector

The TD-GC-FID system is composed of a thermal-desorber (TurboMatrix 650, Perkin Elmer, Inc.) coupled to a gas chromatograph (Clarus 500, Perkin Elmer, Inc.) equipped with an Rxi®-5Sil MS column (60 m, 0,25 mm i.d., film thickness: 0.1 µm, Restek Corporation, Bellefonte, USA) and a flame ionisation detector (FID). The system is also coupled to a mass spectrometer (Clarus 500, Perkin Elmer, Inc.). Analytical method was the same as the method used on the Markes-Agilent TD-GC-MS system. No-recollection was performed for analytical development. Compounds separation was achieved with the following temperature program: from 40 to 305 °C with a thermal ramp of 10 °C min^{-1}.

2.3 Simulation chambers

2.3.1 INERIS dynamic simulation chamber

The INERIS dynamic simulation chamber consists on a borosilicate glass loop (200 l volume) which has been described elsewhere (Martin et al., 2003; Gonzalez-Flesca and Frezier, 2005). It has been especially designed to generate single or multi-component gaseous species atmospheres at known and stable concentrations (from hours to weeks). Clean and dry air is generated by a zero air generator (Claind, AZ Air purifier 2010) and atmospheres are generated by continuous dilution of concentrated mixture (typically, standard pollutants gas tanks). Dilution process is controlled and monitored by mass flow meters. If required, relative humidity is generated from a pressurized bulb containing ultrapure water (18.2 MΩ, ElgaPureLab Flex, Veolia water) connected to a heated liquid mass flow controller system. Temperature was maintained around 22 °C into the chamber by the circulation into the chamber double walls

AMTD
5, 1153–1231, 2012

of a temperature conditioned mixture of water/ethylene glycol. Temperature, pressure and relative humidity are continuously monitored.

2.3.2 CESAM atmospheric simulation chamber

The CESAM atmospheric simulation chamber was used to perform determination of breakthrough volumes presented Sect. 3.2.4. It has been described in detail elsewhere (Wang et al., 2011). Briefly, this facility consists of a cylindrical 4.2 m^3 stainless steel chamber. The chamber is evacuable thanks to a powerful pumping system which combines root pump, rotary pump and turbomolecular pump which allows the evacuation down to 8×10^{-4} mbar between each experiment helping in minimizing memory effect. Both temperature and relative humidity are measured thanks to a HMP234 Vaisala® humidity and temperature transmitter equipped with a capacitive thin-film polymer sensor Humicap®.

Compounds injection is performed introducing a precisely known pressure (in the range 0.1 mbar) via a vacuum ramp from a pure standard frozen solution into a bulb of known volume (V = 1.0832 l). The bulb content is then immediately flushed into the chamber.

Hydrocarbons products were monitored using Fourier Transform InfraRed spectrometry (FTIR) from Bruker GmbH. The total optical pathlength for the in-situ FTIR measurement was set to 192 m.

2.3.3 EUPHORE simulation chamber

Simulation chamber experiments on limonene ozonolysis (cf. Sect. 4) and isoprene photo-oxidation (cf. Sect. 3.3.4) were conducted in the chamber B of the EUphore PHOtoREactor (EUPHORE) facility in Valencia (Spain), consisting of ~200 m^3 outdoor hemispheric Fluorinated Ethane/Propene (FEP) bags mixed with high power fans. For limonene ozonolysis experiment the chamber was protected from outdoor conditions (irradiation) by a retractable steel cover to achieved dark experiment. Before

AMTD
5, 1153–1231, 2012

experiment, the chamber was flushed overnight, and then filled, with clean air from an air purification system including absorption dryer with molecular sieve. Air volume losses due to sampling were compensated by clean air introduction. Prior every experiment, an aliquot of SF_6 was introduced in the chamber as an inert tracer to determine the dilution rate. Limonene or isoprene was introduced under heated clean air stream. Relative humidity was generated by water introduction through a sprayer. Humidity and temperature were monitored by a hygrometer model TS-2 (Waltz, Effeltrich, Germany). Pressure was monitored by a barometer model Air DB-VOC (Sirsa, Madrid, Spain). Ozone was produced by passing clean air (Linde, purity of 99.999 %) through a bulb equipped with a mercury UV lamp. This home-made system was previously calibrated as producing ozone with a typical rate of 20 ppb min^{-1}.

Terpenes concentration was monitored by an on-line gas chromatograph coupled with photoionisation detector (Fisons GC-8160, Thermo-Fisher, Waltham, MA, USA equipped with a DB-624 cyano-propylphenylpolysiloxane fused silica capillary column, J & W Scientific, 30 m, 0.32 mm i.d., 1.8 µm film) programmed isothermally at 160 °C with a total run of 10 min. Total aerosol mass is continuously monitored by a TEOM microbalance (model 1400a, Rupperch and Patashnick Co. Inc, Albany, USA) with a one minute averaging time step.

3 Analytical development

3.1 Method overview

The method development is based on the simultaneous sampling of gaseous phase on Tenax TA sorbent tubes pre-coated with the derivatisation agents and particulate phase on filters (derivatised after sampling). Global sampling and analytical method is summarized Fig. 3.

The method allows the use of common VOCs denuders upstream aerosols collection filters. Nevertheless, in the present analytical development no denuder was tested.

AMTD
5, 1153–1231, 2012

3.2 Carbonyl functions derivatisation in gas phase samples

For the analysis of carbonyl bearing molecules in the gas phase, air samples collection is achieved on Tenax TA sorbent tubes pre-coated with PFBHA. As the derivatisation reaction occurs onto the sorbent of the cartridges which is not a classical medium for such a chemical reaction classical, one of the key parts of this work was the optimisation of this process and its characterization.

3.2.1 Sorbent coating and derivatisation

Tenax TA coating is achieved in 20 min, without any solvent by PFBHA sublimation: a nitrogen stream (100 ml min^{-1} $tube^{-1}$) flows through a glass bulb containing solid PFBHA connected to one or more Tenax TA sorbent tubes (max. 8 tubes, Fig. 4). A PFBHA mass of 330 µg (1.3 µmol) per tube connected is introduced. For a 12 l sample volume (corresponding to a sampling flow rate of 100 ml min^{-1} for 2 h), this PFBHA mass is sufficient to derivatise (i.e. is 10 times higher than) a carbonyl compound concentration of around 1 mg m^{-3} (for a mean molecular weight of 100 g mol^{-1}). Glass bulb and sorbent tubes are maintained at 110 °C in an oven during the coating. As shown by Ho and Yu (2002), after sampling, closed samples are stored at room temperature for a minimum of five days before TD-GC-MS analysis to allow full derivatisation.

3.2.2 Humidity influence

3.2.3 Derivatisation yield and standards realisation

Derivatisation yield was estimated comparing in solution derivatisation and on-Tenax TA derivatisation. Standard solutions were prepared in a 5/95 water/acetonitrile mixture at a concentration of 80 ng $µl^{-1}$ with 19 carbonyl compounds (11 aldehydes: methacrolein, valeraldehyde, 2-ethylbutyraldehyde, benzaldehyde, nonanal, ethyl-3-methyl-4-oxocrotonate, citronellal, citral, glyoxal, perillaldehyde, glutaraldehyde; 7 ketones: butanone, 3-buten-2-one, 4-heptanone, carvone, 2,3-butadione,

AMTD
5, 1153–1231, 2012

3-methyl-2,4-pentadione, camphor; 1 keto-aldehyde: methylglyoxal). For in solution derivatisation, a molar excess of PFBHA corresponding to ten times the molar concentration of derivatisable functions was added per 1 ml of each solution. The solutions were let at room temperature (around 22 °C) for 24 h. One micro litre of each of the five derivatised solutions was subsequently vaporized under heated helium stream (270 °C) and trapped onto five clean Tenax TA tubes just before TD-GC-FID analysis. For on-sorbent derivatisation, one micro litre of the previous non derivatised solutions was injected onto PFBHA coated Tenax TA tubes by the same way. In order to expose the tubes to humidity, a clean and wet (50 % RH) zero air was sampled onto the tubes during 30 min at a flow rate of 100 ml min^{-1}. Samples were let at room temperature for 5 days before TD-GC-FID analysis. Two on-Tenax TA derivatisations per solution were performed. Comparison results are shown on Fig. 7. For aldehydes (Fig. 7a), on-Tenax TA derivatisation results present close to 100 % or higher yields (from 102 % to 205 %) compared to in solution derivatisation, except for methacrolein (9 %). For ketones (Fig. 7b), on-Tenax TA derivatisation results present lower yield (from 12 % to 41 %) compared to in solution derivatisation (derivatised camphor was not observed in both derivatisation processes).

Based on this experiment and previous (see Sect. 2.2.2), repeatability was estimated from the standard deviation/mean ratio and determined to be equal to or lower than 10 % for compounds with more than 4 carbons and lower than 20 % for compounds with 4 carbons or less (except for the 80 % RH experiment). Thus, despite low derivatisation yields for some compounds, satisfactory on-Tenax TA derivatisation repeatability was observed, allowing quantification.

Consequently, calibration method for quantification cannot be based on standards prepared from in solution derivatisation but has to be achieved by preparing standards reproducing real sampling conditions with the method described just above and used for on sorbent derivatisation yield estimation (non derivatised standard solutions are injected onto PFBHA coated Tenax TA tubes and exposed to a wet zero air stream to bring humidity).

AMTD
5, 1153–1231, 2012

3.2.4 Breakthrough volumes

Experiments to determine breakthrough volumes have been performed in the CESAM smog chamber. Relative humidity was maintained between 65 and 80 % as it was assumed to be unfavourable conditions for breakthrough volumes which may lead to the determination of a lower limit. A temperature of 23 °C remained constant during experiment. Samplings were achieved on five sampling trains of two in series identical PFBHA coated sorbent tubes at a flow rate of 100 ml min^{-1}. Experiment was achieved within five hours. One sampling was stopped each hour in order to test five sampling volumes.

Breakthrough volume is defined as the air volume required to completely elute a compound through an adsorbent tube (Baltussen et al., 2002). It defines a limit beyond which the trapping is no more fully efficient and where losses may be encountered. It is defined for a given compound on a given mass of adsorbent and in given environmental conditions of temperature and relative humidity (CEN, 2005). Breakthrough volumes for PFBHA coated Tenax TA sorbent tubes were evaluated for a series of five carbonyls compounds. A mixture of methacrolein, hydroxyacetone, octanal, benzaldehyde, carvone and perillaldehyde was injected in the CESAM simulation chamber with respective concentrations of 71.0, 78.4, 121.5, 100.6, 137.4 and 152.2 µg m^{-3}. Absolute quantification of these species was achieved by the method used for their injection: for each one of them, a precisely known pressure (in the range 0.1 mbar) was introduced via a vacuum ramp from a pure standard frozen solution into a bulb of known volume (V = 1.0832 l). The bulb content was then immediately flushed into the chamber.

For a given compound, breakthrough volume is reached when measurable quantities of this compound are found in the second coated tube (back-up tube). Results are shown on Fig. 8. For most of the compounds breakthrough were found satisfactory as it fall in the range of what is needed to sample organics in air. For methacrolein, breakthrough volume was reached within the first hour, corresponding to a sampling volume smaller than 6 l. It was reached between the first and the second hour for

AMTD
5, 1153–1231, 2012

hydroxyacetone corresponding to a breakthrough volume between 6 and 12 l. Nevertheless, for the others compounds, octanal, benzaldehyde, carvone and perillaldehyde, breakthrough volumes were not reached within the five hours corresponding to a breakthrough volume higher than 30 l (results are only shown for perillaldehyde example, Fig. 8c). Consequently, when the method was applied, a sampling time between one and five hours was used depending on atmosphere concentrations but keeping in mind that carbonyls with a number of carbon inferior to five are subjected to breakthrough, i.e. keeping back-up tubes if C_1-C_4 carbonyl compounds require quantification.

3.2.5 Linearity and detection limits

Both linearity and detection limits were evaluated from calibration curves. A dilution series of 5 carbonyl compounds solutions (9 aldehydes and 8 ketones) from 5 to 320 ng μl^{-1} was used. Calibration curves were performed from standards reproducing real on-Tenax TA sampling conditions (see Sect. 3.2.3). Results are shown Table 1 where calibration curves slopes, good correlation coefficient (ranging from 0.9883 and 0.9999) and satisfactory detection limits are given. Response linearity was evaluated from a specific *m/z* ion extraction for each compound and was statistically validated (Student's t-test). For the negative intercepts obtained for two compounds (citronellal and citral), no explanation has been found. Uncertainties (corresponding to ±2 standard errors) are given for a 95 % confidence level. Detection limits (corresponding to 3 times the area noise) are given in absolute mass per sample tube and in concentration units for a sampling volume of 12 l (i.e. 100 ml min^{-1} for 2 h). They range from 0.07 to 6 ng per tube corresponding to concentrations ranging from 6 to 500 ng m^{-3} (or 1.3 to 81 ppt). These detection limits are in the same order of magnitude or better than those obtained by Ho and Yu (2004) and Li et al. (2009) which proposes sampling aldehydes onto PFPH (pentafuorophenyl hydrazine) coated Tenax TA tubes and respectively obtained detection limits ranging from 0.07 to 6 ng sampled per tube (corresponding to atmospheric concentrations ranging from 6 to 500 ng m^{-3} for 12 l sample volume).

AMTD
5, 1153–1231, 2012

Compared to the classical DNPH method, involving carbonyls collection onto DNPH-coated silica cartridges before elution and analysis by HPLC-UV, these detection limits correspond to a gain of around one order of magnitude (Ho and Yu, 2004). The ppt detection limits order of magnitude provided by the method are more than satisfactory considering the carbonyls concentration levels which can be reached in the atmosphere. As an example, Müller et al. (2006) found biogenic carbonyl compounds concentrations in a forest region to be about the hundreds of ppt.

3.3 Acid and hydroxyl functions derivatisation in gas phase samples

For the analysis of OH bearing gaseous molecules, gas phase collection is performed on Tenax TA sorbent tubes pre-coated with MTBSTFA reagent in order to analyse the carboxyl and hydroxyl containing fraction of the gaseous organic matter. This reaction requires significantly different experimental condition from PFBHA derivatisation and is known to be sensitive to different parameters. In particular, it is sensitive to humidity. It has, hence, required the development of a specific protocol.

3.3.1 Sorbent coating and post-sampling derivatisation protocol

Similarly to the PFBHA procedure, Tenax TA coating with MTBSTFA is achieved without any solvent by vaporisation of 0.3 µl pure MTBSTFA (+1 % TDBMCS) under a heated helium stream (270 °C, 30 ml min^{-1}) for only 8 min. A dry purge of 2 min is applied before MTBSTFA injection to remove traces of water on the sorbent tube. However, as previously said, MTBSTFA and MTBSTFA derivatives are subjected to hydrolysis, especially during sampling of humid real or simulated atmospheres. Consequently, in order to promote derivatisation, and considering Tenax TA hydrophobia, samples are re-exposed to MTBSTFA after sampling: samples are opened, 0.3 µl of pure MTBSTFA (+1 % TDBMCS) are spiked at each end of the sampling tubes and the re-closed samples are let in a furnace at 60 °C for 5 h. After cooling to room temperature, samples

AMTD
5, 1153–1231, 2012

must be rapidly analysed by TD-GC-MS within 5 h to prevent derivatives decomposition.

3.3.2 Derivatisation yield and standards preparation

Derivatisation yields were estimated comparing in solution derivatisation and on-Tenax TA derivatisation. In solution derivatisation was achieved at room temperature for two hours adding a molar excess of MTBSTFA (corresponding to ten times the molar concentration of derivatisable functions) to the non derivatised solution in acetonitrile (80 ng μl^{-1}). Derivatised solutions were then vaporized under heated helium stream and trapped onto clean Tenax TA tubes before TD-GC-FID analysis. On-Tenax TA derivatisation was achieved preparing standard Tenax TA tubes. Clean Tenax TA tubes were spiked with the not-derivatised solution directly into the Tenax TA adsorbent with a micro-syringe. Spiked tubes were placed 3 min under a heated helium stream (270 °C, 30 ml min^{-1}) in order to elute compounds on the Tenax surface and better represent a real sampling. Tubes, thereafter referred as carboxyls/hydroxyls standard tubes, were then derivatised as previously presented for samples (see Sect. 3.3.1) and analysed by TD-GC-FID. Comparison results are shown Fig. 9. They reveal good agreement between in solution and on-Tenax TA derivatisation yield for the acids while significant discrepancies are observed for hydoxy bearing species. This is especially true for some alcohols such as phenol, tert-butyl-4-hydroxy butyrate, 1-nonanol, 4-methoxyphennol - for which decreases larger than 45 % in the derivatisation yield.

Thus, despite low derivatisation yields for some compounds, satisfactory on-Tenax TA derivatisation repeatability was observed, allowing quantification.

Consequently, calibration method for quantification cannot be based on standards prepared from in solution derivatisation but has to be achieved by preparing standards reproducing real sampling conditions with the method described just above and used for on sorbent derivatisation yield estimation.

AMTD
5, 1153–1231, 2012

3.3.3 Humidity influence

The ability of the post-sampling derivatisation process to overcome humidity influence on the derivatisation process was evaluated bringing humidity on carboxyl/hydroxyl standard tubes before post-derivatisation process. Two series of three carboxyls/hydroxyls standard tubes were prepared spiking one microliter of a non derivatised solution at a concentration of 80 ng μl^{-1}. A wet zero air (50 % RH) was sampled for thirty minutes at a flow rate of 100 ml min^{-1} on the first series while the second series remains closed, in dry conditions. After post-derivatisation process, both series were analysed by TD-GC-FID. Results are shown on Fig. 10 and reveal no significant discrepancies between wet and dry standards (except from nonanol and phenol) despite a lower repeatability for some compounds in wet conditions. Consequently, post-derivatisation process is assumed to overcome humidity influence on the analytical protocol and calibration can be performed from dry carboxyls/hydroxyls standard tubes.

From the humidified series of 3 standards, an estimation of the method repeatability can be given. The mean standard deviation/mean ratio was 25 % for all compounds, ranging from 12 (tertbutyl-4-hydroxybutyrate) to 55 % (ethylene glycol) for alcohols and from 1 (crotonic acid) to 79 % (caffeic acid) for carboxylic acids.

3.3.4 Breakthrough volumes

Given the difficulty to generate stable atmospheres of low vapour pressure hydroxyl and carboxyl compounds, precise breakthrough volumes could not be determined. An evaluation of MTBSTFA coated sorbent tubes breakthrough is given here as breakthrough data for a series of carboxyl and hydroxyl compounds identified from the isoprene photo-oxidation experiment achieved in the EUPHORE chamber since this experiment produced a wider range of volatile oxygenated species compared to the limonene ozonolysis experiment. Initial isoprene concentration was 55 ppb for an initial H_2O_2 concentration of 4 ppm. Relative humidity and temperature were respectively

AMTD
5, 1153–1231, 2012

25 % and 303 K during sampling time, after chamber opening to sunlight and system stabilisation. Sampling was achieved onto two in series MTBSTFA pre-coated Tenax TA sorbent tubes at a flow rate of 100 ml min^{-1} during two hours (sampled volume: 12 l). Second tube (following air flux) is considered as a "back-up tube" to collect the compounds which have not been completely trapped on the first one. Results are shown Table 2 which gives an evaluation of the breakthrough in %, corresponding to the ratio between what is measured in the back-up tube and what is measured in the sample tube, for each studied compounds. No breakthrough can be observed for most studied compounds especially for those bearing several functionalities and/or displaying a carbon skeleton with more than five carbons.

It must be pointed out, to explain the measurement of compounds with more than five carbons when running an isoprene photo-oxidation experiment, that the smog chamber blanks were contaminated. Since the purpose of this experiment was to determine breakthrough volume and not to explain isoprene oxidation pathways, all the detected compounds have been taken into account for breakthrough evaluation.

Significant breakthrough is only observed for mono-functionalised compounds with a carbon number less than seven. If these compounds are targeted, the use of back-up tubes is required. Poly-functionalised compounds, even with only two carbons, do not seem to be affected by breakthrough, in these particular experimental conditions. Their breakthrough volumes are consequently estimated to be greater than 12 l. When performing measurement in that type of sampling conditions of samples volume, sampling flow rate, humidity and temperature, the use of back-up tubes is not required. When performing measurements in different conditions, determination of breakthrough volumes or use of back-up tubes are recommended.

3.3.5 Linearity and detection limits

Both linearity and detection limits were evaluated from calibration curves. A dilution series of 5 hydroxyl compounds and organic acids solutions (of 6 alcohols and 14 organic acids) from 5 to 320 ng μl^{-1} was used. Calibration curves were performed from

AMTD
5, 1153–1231, 2012

standards reproducing real on-Tenax TA sampling conditions (see Sect. 3.3.2). 1 µl of carbonyl compounds standard solutions were spiked into Tenax TA tubes and subsequently derivatised by MTBSTFA exposition at 60 °C for 5 h. Results are shown Table 3. Response linearity for all compounds was statistically validated (Student's t-test) and uncertainties (corresponding to ±2 standard errors) are given for a 95 % confidence level. Detection limits (corresponding to 3 times the area noise) are given in absolute mass per sample tube and in concentration units for a sampling volume of 12 l (i.e. 100 ml min^{-1} for 2 h). They range from 0.05 to 10 ng per tube and from 5 to 834 ng m^{-3}.These detection limits are lower than those obtain by Wu et al. (2008) for volatile fatty acids analysis without derivatisation and in the same order of magnitude or lower than those obtained by Chiappini et al. (2006) or Pietrogrande et al. (2010) ranging from 1.2 to 6.8 ng per GC-MS injection for mono and di-carboxylic acids detection in the aerosol phase with previous derivatisation process respectively in CO_2 super-critical fluid and in solution. The detection limits ranging from 1 to 232 ppt are more than satisfactory to measure hydroxyl and carboxyl compounds whose concentration levels are several orders of magnitude below. As an example, dicarboxylic acids concentration levels measured by Legrand et al. (2005) on altitude sites in France are a few tens of ppb.

For general purpose, PFBHA derivatisation is usually achieved in aqueous or water-containing solution (Cancilla and Que Hee, 1992) and a molecule of water is formed for each derivatised compound (Fig. 5). A positive influence of the humidity contained in the sampled air is consequently expected on the derivatisation process. On another hand, humidity can disturb compounds collection reducing the adsorption efficiency (Harper, 1993; Loedwyckx and Vansant, 2000). In order to evaluate this humidity influence a series of aldehydes was sampled from dry (0 % RH) and wet (50 % RH) simulated atmosphere. The experiment was carried out in the INERIS dynamic simulation chamber. The system is adjusted to generate crotonaldehyde, benzaldehyde, butanal, pentanal and hexanal at respective concentrations of 11.7, 17.7, 12.0, 14.3, and 16.7 µg m^{-3}. Sampling was performed during four hours at a sampling flow rate

AMTD
5, 1153–1231, 2012

of 150 ml min^{-1}, connecting coated sorbent tubes to the chamber through a sampling cane. Five and six replicates were respectively performed forA complementary experiment was achieved in order to evaluate bias linked with humidity variations within a realistic relative humidity range. Three sampling series of three replicates were achieved at 30, 50 and 80 % RH. Sampling was performed during one hour at a sampling flow rate of 100 ml min^{-1}. Results are shown Fig. 6. They reveal no significant bias linked to humidity variations within this realistic relative humidity range. A relative humidity of 30 % appears to be sufficient to reach maximum derivatisation yield in these conditions. However, a slight repeatability decrease is observed at 80 % RH, probably due to competition between water and adsorbed organic molecules on adsorbent surface sites. Nevertheless, this observation is consistent with the fact that high humidity levels are known to affect sampling on classic adsorbents, decreasing breakthrough volumes for example (Harper, 1993; Loedwyckx and Vansant, 2000). The developed method to trap and derivatise gaseous carbonyl compounds is consequently considered as suitable under realistic sampling conditions.

A complementary experiment was achieved in order to evaluate bias linked with humidity variations within a realistic relative humidity range. Three sampling series of three replicates were achieved at 30, 50 and 80 % RH. Sampling was performed during one hour at a sampling flow rate of 100 ml min^{-1}. Results are shown Fig. 6. They reveal no significant bias linked to humidity variations within this realistic relative humidity range. A relative humidity of 30 % appears to be sufficient to reach maximum derivatisation yield in these conditions. However, a slight repeatability decrease is observed at 80 % RH, probably due to competition between water and adsorbed organic molecules on adsorbent surface sites. Nevertheless, this observation is consistent with the fact that high humidity levels are known to affect sampling on classic adsorbents, decreasing breakthrough volumes for example (Harper, 1993; Loedwyckx and Vansant, 2000). The developed method to trap and derivatise gaseous carbonyl compounds is consequently considered as suitable under realistic sampling conditions.

AMTD
5, 1153–1231, 2012

3.4 Carbonyl functions derivatisation in particulate phase samples

Particulate phase collection for carbonyl compounds analysis is achieved on 47 mm quartz fibre filters (see Sect. 2.1.4) at a typical flow rate of 1 $m^3 h^{-1}$ (16.7 $l min^{-1}$) simultaneously with gaseous phase sampling. PFBHA post-sampling derivatisation process is performed by sample introduction in stainless-steel tubes suitable for thermal-desorption and sample exposition to in solution PFBHA. Humidity influence on particulate phase derivatisation process is expected to be similar to what has been observed for gas phase derivatisation (cf. Sect. 3.2.2).

3.4.1 Post-sampling derivatisation protocol

47 mm sample filter is cut in four parts and totally introduced into a clean stainless steel thermal desorption tube. After the introduction of each quarter, 2 µl of a saturated PFBHA solution (27 mg ml^{-1}, 90/10 acetonitrile/ultrapure water mixture) is deposed onto the new introduced filter part. A glass bulb with 8 outlets is then used to expose in-tube samples to saturated PFBHA aqueous solution for 40 h since this duration is expected to be sufficient to impregnate rolled filter with PFBHA and is convenient for protocol organisation. From one end, filter sample tubes are connected to the bulb outlets while the other end is maintained closed.1 mL of ultrapure water is introduced in the bulb and stirred (500 rounds per min). 90 mg of pure and solid PFBHA is then added to the water. The bulb is closed and the system is let at room temperature. After 20 h, filter sample tubes are disconnected, reversed, reconnected by the other end and let for 20 h again. Filter sample tubes are then definitely disconnected, closed and kept at room temperature for a minimum of 5 days before analysis.

3.4.2 Standard preparation, linearity and detection limits

Standards used to achieve calibration curves were prepared and derivatised in the same way as sample filters. Clean quartz fibre filters are introduced into empty

AMTD
5, 1153–1231, 2012

stainless steel desorption tube with deposition of PFBHA saturated solution, spiked with 1 µl of standards carbonyl compounds solutions (5 points from 5 to 320 ng µl^{-1}) and let 40 h connected to a stirred glass bulb containing 1 ml of PFBHA saturated aqueous solution (with tube reversion after 20 h) at room temperature. Both linearity and detection limits were evaluated. Results are shown Table 4 giving for each compound the calibration curve slopes, the correlation coefficients which are globally good (most are ranging from 0.9131 and 0.9999 except for three compounds displaying R^2 ranging from 0.7846 to 0.8890), and the detection limits which are satisfactory.

Response linearity for all compounds was statistically validated (Student's t-test) and uncertainties (corresponding to ±2 standard errors) are given for a 95 % confidence level. Detection limits (corresponding to 3 times the area noise) are given in absolute mass per filter and in concentration units for a sampling volume of 2 m^3 (i.e. 16.7 l min^{-1} for 2 h). These detection limits ranging from 0.04 to 120 ng per filter (corresponding to a atmospheric concentration of 0.02 and 60 ng m^{-3} for a 2 m^3 sample volume) are more than sufficient to measure carbonyl compounds in the atmosphere where their concentrations are in the same order of magnitude (Liggio and McLaren, 2003).

3.5 Acid and hydroxyl functions derivatisation in particulate phase samples

Particulate phase collection for carboxyl and hydroxyl compounds analysis is achieved on 47 mm Teflon-quartz fibres filters (see Sect. 2.1.4.) at a typical flow rate of 1 m^3 h^{-1} (16.7 l min^{-1}) simultaneously with gaseous phase sampling. MTBSTFA post-sampling derivatisation process is performed after sample introduction in stainless-steel tubes suitable for thermal-desorption by samples exposition to pure MTBSTFA (+1 % TDBMCS).

3.5.1 Post-sampling derivatisation protocol

47 mm sample filter is cut in four parts and totally introduced into a clean stainless steel thermal desorption tube. MTBSTFA is not spiked directly onto the filter. 10 µl of

AMTD
5, 1153–1231, 2012

pure MTBSTFA (+1 % TDBMCS) are introduced in the bottom of one tube cap and the sample filter tube is closed in vertical position above the MTBSTFA (cf. Fig. 11). Filter exposition to MTBSTFA is achieved at room temperature during 24 h. Filter sample tube is then directly analysed in TD-GC-MS within 5 h.

3.5.2 Humidity influence and standard preparation

As for gaseous compounds derivatisation on Tenax TA tubes, humidity is expected to influence on-filter MTBSTFA derivatisation process and Teflon-quartz filters were chosen to reduced moisture loading during wet air sampling. Nevertheless, in order to evaluate the influence of this moisture loading on the derivatisation process, response factors of a series of standard compounds were compared from dry and pre-humidified Teflon-quartz filters. Five points calibration curves (from 5 to 320 ng μl^{-1}) were achieved from standards filters prepared and derivatised in the same way as sample filters. Wet Teflon-quartz filters were humidified sampling wet zero air (50 % RH) at 7 l min^{-1} for 2 h. Clean and dry or wet filters were introduced into empty stainless steel desorption tubes and spiked with standards solutions. They were subsequently derivatised by exposition to MTBSTFA for 24 h at room temperature. Compounds response factors comparison results are given Fig. 12. Surprisingly, response factors were significantly higher onto humidified filters for 15 standard compounds on 18. Moreover, for keto-acids (6-oxoheptanoic acid, cis-pinonic acid), di-acids (succinic acid, pinic acid) and malic acid, compounds responses became linear compared to their responses on dry filters (not mentioned on Fig. 12). The reason why humidity positively influences on-filter derivatisation is not clear. It might be explained by competition phenomena between water and polar compounds to form bonds with quartz surface. In this case, moisture loading may improve both derivatisation reaction and desorption capacity limiting polar compounds bonding with filter surface. Anyway, positive influence of filters moisture loading has two main consequences on the method: it is not necessary to dry sample filters before MTBSTFA derivatisation and calibration curves have to be achieved onto humidified Teflon-quartz filters.

AMTD
5, 1153–1231, 2012

3.5.3 Linearity and detection limits

Both linearity and detection limits were evaluated from calibration curves achievement previously used for humidity influence evaluation. Results are shown Table 5 which gives for each compound the calibration curve slopes, correlation coefficients which are satisfactory, ranging from 0.9433 to 0.9999, and detection low detection limits.

Response linearity was statistically validated (Student's t-test) and uncertainties (corresponding to ±2 standard errors) are given for a 95 % confidence level. Detection limits (corresponding to 3 times the area noise) are given in absolute mass per filter and in concentration units for a sampling volume of 2 m^3 (i.e. 16.7 l min^{-1} for 2 h). Linearity was not validated for two standard compounds, 4-oxoheptanedioic acid (keto-di-acid) and 3-carboxyhexanedioic acid (tri-acid). Nevertheless these compounds were detected above an absolute mass of 100 ng spiked into standard filters and their responses were linear onto Tenax TA tube MTBSTFA derivatisation, meaning that keto-di-acids and tri-acids cannot be quantified but can be detected in the particulate phase. Improvement of the developed particulate phase MTBSTFA derivatisation protocol is required to specifically quantify keto-di-acids and tri-acids. Detection limits for all other compounds range from 0.04 to 1.0 ng per filter. These detection limits are significantly better than those obtain by Chiappini et al. (2006) ranging from 1 to 7 ng for an analogous series of acids, keto-acids and di-acids through BSTFA derivatisation process during supercritical fluid extraction coupled to GC-MS analysis. They are more than satisfactory to measure carboxylic acids in atmospheric particles since their concentrations level are about a few tens of ng m^{-3} as measured by Sun and Ariya (2006).

4 Method application to limonene ozonolysis in simulated atmosphere

Limonene is a significant contributor to monoterpenes emissions that accounts for around 11 % of global VOCs emissions (Guenther et al., 1995). Moreover, with two double bonds, it is more reactive and has a higher SOA yield (around two time, Griffin

AMTD
5, 1153–1231, 2012

et al., 1999) compared to mono-unsaturated monoterpenes, such as α- and β-pinene, more emitted at a global scale. Limonene is consequently supposed to be a significant contributor to SOA at global scale. Furthermore, limonene is also widely present in indoor environments as it is largely employed in household cleaning product, air freshener or essential oil for example (Singer et al., 2006). Limonene oxidation in indoor environment, especially through ozonolysis, has been demonstrated by many studies in the last years, pointing out strong airway irritants and ultrafine particles formation (Clausen et al., 2001; Sarwar and Corsi, 2007; Langer et al., 2008; Coleman et al., 2008; Forester and Wells, 2009; Jardine et al., 2011).

Therefore, limonene ozonolysis was chosen as a relevant system to assess the ability of the developed method to explore the chemical composition of the oxygenated secondary organic matter simultaneously in gaseous and particulate phases. Moreover, this chemical system is sufficiently well characterized, allowing us to compare our results to literature for method validation purpose (e.g. Leungsakul et al., 2005a,b; Jaoui et al., 2006; Walser et al., 2007; Forester and Wells, 2009; Yasmeen et al., 2011).

4.1 Experimental protocol

Limonene ozonolysis experiment was conducted in the EUPHORE simulation chamber (cf. Sect. 2.3.3) in order to approach real indoor or outdoor atmosphere conditions. Limonene was first injected in the chamber at an initial concentration level of 100 ppb. Non acidified sulphate ammonium seeds were introduced by nebulisation of a 0.02 M solution at a concentration of 12.5 $\mu g\,m^{-3}$. Water was then introduced until an initial relative humidity of 50 % was reached. Ozone was finally injected during 5 min 16 s, corresponding to an initial concentration of 105 ppb (see Sect. 2.3.3). Mean temperature during experiment was 300 ± 1 K. No hydroxyl radical scavenger was introduced as this would stray experiment from realistic indoor conditions (Docherty and Ziemann, 2003; Jonsson et al., 2008). Main parameters variations as monitored during the course of the experiment are given (Fig. 13).

AMTD
5, 1153–1231, 2012

In order to evaluate the fraction of oxidative chemistry initiated by hydroxyl radicals on limonene – coming from Criegee intermediate decomposition after ozone addition onto double bonds – simulation was run using the Master Chemical Mechanism, MCM v3.2 (Jenkin et al., 1997; Saunders et al., 2003). Initialising the MCM with our experimental conditions it was found that around two-third of initial limonene amount reacts with ozone while one-third is expected to react with hydroxyl radicals. As a result, both ozonolysis and photo-oxidation products of limonene are likely to be detected and consequently specifically researched.

Blanks were sampled just before ozone introduction during 120 min. Gas phase blanks were sampled on one PFBHA and one MTBSTFA coated Tenax TA tubes at a flow rate of 100 ml min^{-1} downstream a Teflon filter (Zefluor, 47 mm, Pall Life Sciences). Particulate phase blanks were sampled in parallel on one quartz filter and one Teflon-quartz filter at a flow rate of 16.7 l min^{-1}. Sampling was achieved during 160 min after ozone introduction and system stabilisation (aerosol maximum mass reached within one hour). Gas phase was sampled onto three PFBHA and three MTBSTFA coated Tenax TA tubes at a flow rate of 100 ml min^{-1} downstream a Teflon filter. For each derivatisation reagent one tube is equipped with a back-up tube (see Sect. 3.2.4) likewise coated to observe possible breakthrough of the sample tubes. Particulate phase was sampled onto one Teflon-quartz and two quartz filters at a flow rate of 16.7 l min^{-1}. No VOC denuder was used in this method testing experiment. It is important to note that no specific set-up was used to minimise sampling artifact for these experiments. Indeed, the main objective of the work here was the application of the methodology presented and characterised in the previous section.

All samples were analysed by TD-GC-MS, in both EI and CI mode, as previously described (see Sect. 2.2.).

AMTD
5, 1153–1231, 2012

4.2 Results

4.2.1 Aerosol mass yield

Secondary aerosol from limonene ozonolysis growth curve is given Fig. 14. It corresponds to the time dependant aerosol mass yield Y calculated from TEOM measurements and defined as:

$$Y = \frac{\Delta M_0}{\Delta HC}$$

where ΔM_0 is the aerosol mass loading ($\mu g\,m^3$) and ΔHC is the total reacted limonene ($\mu g\,m^3$), both corrected from dilution and wall losses. Final aerosol mass yield was around 20 %. Higher values are usually observed in the same experimental conditions (~50 % by Jaoui et al., 2006; Northcross and Jang, 2007; Sun et al., 2011, ~65 % by Saathoff et al., 2009). The lower value measured here can be explained by the elevated temperature of 300 K achieved in the chamber during experiment as shown by Saathoff et al. (2009) studying the influence of temperature on SOA yields from limonene ozonolysis.

4.2.2 Product detection and identification

Compound detection and identification are based on characteristic fragmentation pattern of PFBHA and MTBSTFA derivatives (cf. Table 6) in EI and CI modes. As much as possible, compound spectra and retention time were compared to available standard data. Compounds are positively identified in the only cases where standard are available. Otherwise, a tentative assignment is proposed based on characteristic fragmentation and retention time comparison vs. surrogate standards. Compounds detected in chamber blanks in the same order of magnitude than in samples were removed from the product list.

Around 30 compounds can be detected in the gas phase as PFBHA or MTBSTFA derivatives products (20 PFBHA derivatives and 10 MTBSTFA derivatives) and

AMTD
5, 1153–1231, 2012

around 65 in the particulate phases (30 PFBHA derivatives and 35 MTBSTFA derivatives). These products range from C_3 to C_{10} and from mono to tri functionalized species. In the gas phase detected compounds range from C_3 mono-carbonyl, C_5 mono-hydroxyl or C_6 mono-acid to C_{10} di-carbonyl and C_8 di-hydroxyl or di-acid. In the particulate phase tri-functionalised compounds are observed until C_8–C_{10}.

Among all these detected products, 25 have been positively (based on standard mass spectra comparison) or tentatively identified (based on surrogate standard and/or mass spectra). An overview of the limonene oxidation products detected and tentatively or positively identified in both gas and particulate phases is presented on Table 7. Fourteen products previously identified from limonene oxidation experiments (Leungsakul et al., 2005a; Jaoui et al., 2006; Forester and Wells, 2009) or expected from theoretical oxidation scheme (Leungsakul et al., 2005b) were observed (P2, P3, P5, P6, P8, P9, M1, M2, M4, M6, M7, M9 and M10).

In addition to these species, eleven other products were detected for the first time to our best knowledge (P1, P7, M4, M6, M9, M12, M13, M14, M15, M16 and M17).

This provides certainly the most comprehensive list of detected compounds in a single experiment for limonene ozonolysis in both gaseous and particulate phases.

All these new information show the method capacity to explore the chemical composition of the secondary organic matter in a relevant range of semi-volatile compounds and hence potentially open the way to new chemical scheme building for the semi-volatile organic species production in the limonene ozonolysis system. An example of chromatograms is given for the analysis of carbonyl compounds in both phases (Fig. 15).

Recollection is a useful option provided by some of commercial thermal desorbers which provide a way to easily obtain complementary data for compounds identification by the re-injection of the same sample. We used it here to confirm peak identification by re-injecting our analytes in chemical ionization mode. It must be indicated here that this approach is affected of an elevated detection limits obtained in CI mode for recollected samples, especially for MTBSTFA derivatised samples. It is obviously not validated for

AMTD
5, 1153–1231, 2012

quantification as further experiments have shown that recollected MTBSTFA samples have to be analyzed as soon as possible after first injection. Unfortunately, this was not possible for this study. Other attempts have shown that a 24 h delay seems to significantly improve detection limits compared to the presented recollected sample results, analyzed in CI mode within 7 days.

4.2.3 Quantification and partitioning coefficients estimation

Among the 30 compounds detected in the gas phase and the 65 compounds detected in the particulate only those which it was achieved a relevant standard calibration in gas and/or particulate phases (see Tables 1, 3, 4 and 5) were quantified. This has led to the quantification of 18 detected compounds which are given Table 8.

For compounds quantified in both gas and particulate phases, it was possible to calculate their experimental partitioning coefficient given in Table 9, considering a total aerosol concentration of $45 \pm 12\,\mu g\,m^{-3}$ that corresponds to the average real aerosol concentration during sampling, not corrected from aerosol losses in the chamber. Uncertainties were calculated on the base of gas phase, particulate phase and aerosol mass quantification uncertainties (calibration curves and TEOM uncertainty). Experimental partitioning coefficients are compared to estimation values calculated from theoretical vapour pressure data estimated from three group contribution methods (Myrdal and Yalkowsky, 1997; Nannoolal et al., 2008; Pankow and Asher, 2008). The following parameters are used for these calculations: an experimental temperature of 300 K, an average molecular weigh in the particulate phase (MW_{om}) of $142\,g\,mol^{-1}$ and an activity coefficient (γ_i) of 1.27. These two last values are taken from simulation results in Leungsakul et al. (2005a). When available, experimental partitioning coefficients are also compared with other experimental values.

Total quantified products represent around 16 % in carbon mass of the reacted limonene. The remaining not quantified mass can be divided in three main groups: (1) non identified compounds that were detected here but not quantified (2) non derivatisable species and (3) high molecular weight compounds such as oligomers.

AMTD
5, 1153–1231, 2012

Limononaldehyde (P6) was the most abundant product in the gas phase, as observed by Leungsakul et al. (2005a) from limonene ozonolysis experiments. However, contrary to this previous work, limononaldehyde was also the most abundant product observed in the particulate phase instead of keto-limononaldehyde. Limononaldehyde experimental partitioning coefficient estimation provides a value, $3.5 \times 10^{-3}\,m^3\,\mu g^{-1}$, three orders of magnitude higher than estimation calculation and two order of magnitude higher than Limononaldehyde experimental partitioning coefficients estimated by Leungsakul et al. (2005a) (around $6 \times 10^{-5}\,m^3\,\mu g^{-1}$).

The second most abundant products in the gas phase were Methyl-Glyoxal and Dimethyl-Glyoxal, Methyl-Glyoxal being also the second most abundant compound in the particulate phase. Experimental partitioning coefficient for Methyl Glyoxal is also three orders of magnitude higher than estimated coefficients. However it is similar to experimental values determined by Ortiz et al. (2010) during field ($3.4 \times 10^{-2}\,m^3\,\mu g^{-1}$) and toluene oxidation smog chamber ($1 \times 10^{-4}\,m^3\,\mu g^{-1}$) experiments.

Another important product detected in both gas and particulate phases was 4-oxopentanal (P5). It was previously detected as a limonene oxidation product only by Forester and Wells (2009). It was also observed at high levels in a forestal atmosphere (180–1570 $ng\,m^3$ in the gas phase and 25–207 $ng\,m^3$ in the particulate phase, Matsunaga et al., 2004) indicating that 4-oxopentanal could be an important SOA contributor. However, its major source is assumed by these authors to be the oxidation of 6-methyl-5-heptene-2-one (6-MHO coming from squalene oxidation). 6-MHO was not observed in the present study suggesting another way for 4-oxopentanal formation that will not be discussed here.

Experimental partitioning coefficient estimation for 4-oxopentanal provides a value 5 orders of magnitude higher than estimation calculation.

Dioxohexanal (P7), 3,6-dioxoheptanal (P8) and keto-limononaldehyde (P9) were only quantified in the particulate phase although their estimated partitioning coefficients predict gas phase concentration higher than $100\,000\,\mu g\,m^{-3}$. More realistically, Leungsakul et al. (2005a) provide experimental partitioning coefficients of

AMTD
5, 1153–1231, 2012

keto-limononaldehyde in the range of 1.41–1.76 × 10^{-3} m^3 μg^{-1}. From these values and keto-limononaldehyde particulate phase concentration estimated in the present study, a gas phase concentration of around 1 × 400 ng m^{-3} could be expected, which is still largely above detection limits achieved for di-carbonyls compounds in the gas phase. From this observation, three hypotheses could be advanced. Firstly, tri-carbonyls compounds may not exist significantly in the gas phase under experimental conditions of this work and keto-limononaldehyde gas phase concentration quantified by Leungsakul and co-workers was either mainly a positive artifact due to volatilisation from the particulate phase or linked to different experimental conditions. Secondly, these compounds are more subjected to negative artifact on gas quantification than di-carbonyl compounds due to adsorption on the Teflon filter placed upstream the adsorbent tubes, this negative artifact increasing as expected when decreasing compound volatility (Volckens and Leith, 2003). Thirdly, tri-carbonyls compounds may not be detectable when sampled onto gas collection Tenax TA tubes due to either derivatisation which may not be complete or desorption limitation. Further experiments based on tri-carbonyl standards are required to infer or invalidate this last hypothesis.

Levulinic acid (M1) is the most important acid observed in the gas phase. Li and Yu (2005) proposed that levulinic acid is an oxidation product of 4-oxopentanal. Limonic acid (M9) is the main acid precisely quantified in the particulate phase with a concentration of 70 ± 10 ng m^{-3}. A keto-diacid (M10: ketolimonic acid), two tri-dicarboxylic acid (M15 and M16) have also been identified in the particulate phase. However, since their standard or surrogate standards calibration curve are not linear, their concentration is estimated on the basis of pinic acid for M10 (160 µg m^{-3}) and malic acid for M15 and M16 (100 µg m^{-3} and 80 µg m^{-3}). Limonic acid experimental partitioning coefficient is in the same order of magnitude than estimation calculation from MY and SIM. However, it is an order of magnitude higher than NAN estimation calculation and experimental values provided by Yu et al. (1999) for other biogenic di-acids: pinic acid, caric acid and sabinic acid, respectively 2.8–3.5 × 10^{-2} µg m^{-3}, 3.3 × 10^{-2} µg m^{-3} and 2.7 × 10^{-2} µg m^{-3} at 306–308 K. Experimental partitioning coefficients of hexanedioic

AMTD
5, 1153–1231, 2012

acid (M6) and pentanedioic acid (M4) are also consistent with theoretical calculations. Experimental partitioning coefficient of succinic acid (M2) is one or two orders of magnitude higher than theoretical calculations.

To conclude, from compounds quantification in both gaseous and particulate phases, partitioning coefficients have been calculated. Differences can be observed in comparison with estimated and other experimental coefficients. Some hypothesis can be proposed to explain these discrepancies: (i) estimated partitioning coefficient are calculated on the basis of estimations that may be wrong which is one of the interest of the method: providing partitioning coefficient obtained under real atmospheric conditions, (ii) reactions occurring in the particulate phase can disturb the equilibrium leading to different partitioning coefficients than expected which is another interest of the method: identifying unsuspected reaction pathways, (iii) sampling positive artifacts on particulate phase quantification since no denuder has been used for particulate phase sampling.

Artifacts seem to be less important on di-acids than on carbonyls compounds. This is consistent with (i) the Teflon-quartz nature of the filter media that is expected to reduce adsorption artifact compared to quartz filter, even if this point is not confirmed by Arp et al. (2007) (ii) the artifact tendency expected to decrease decreasing compounds volatility, from carbonyl compounds to limonic acid (Volckens and Leith, 2003).

5 Conclusions and perspectives

This work has provided a useful new analytical method based thermal-desorption-GC-MS coupling, to explore the secondary organic matter composition at a molecular scale from a global point of view, in both gas and particulate phases. Using separately but in parallel two derivatisation reagents, PFBHA and MTBSTFA, to analyze respectively carbonyls compounds and organic acids and hydroxylated compounds, the method provides the opportunity to explore chemical composition up

AMTD
5, 1153–1231, 2012

to tri-functionalized species. Furthermore, it combines the classical advantages of thermal desorption – solvent free, easy to use and fast – to the possibility to analyze a same sample in both EI and CI modes, providing complementary structural information, through the use of the re-collection option of commercial thermal-desorbers. Method capacity to determine the partitioning behaviour of a wide range of semi-volatile compounds has been demonstrated. Quantification in both gas and particulate phases is indeed validated for mono and di-functionalized species and for hydroxyl di-acids. This is a real progress compared to other techniques designed for compound partitioning studies. Compared to TAG instrument (Isaacman et al., 2011), whose main advantage is based on on-line measurements, the developed method widens the detectable species range to polar and multi-functionalized compounds. Compared to denuder-filter techniques (e.g. Leungsakul et al., 2005a; Temime et al., 2007) it provides a simpler way to study the partitioning of the secondary organic matter, avoiding time consuming and prone to losses solvent extraction steps, with similar detection limits. It is an easy way to systematically assess, in simulation chamber experiments and in the field, partitioning behaviour of semi-volatile compounds and provide a set of data in a wide range of environmental conditions able to help relevant integration of partitioning in models.

In this work, method application to the study of limonene ozonolysis demonstrated the method ability to explore the chemical composition of a complex mixture in both gas and particulate phases, detecting both compounds already known as limonene oxidation products and a range of products detected for the first time: 25 compounds have been positively or tentatively identified, 9 being in both gaseous and particulate phases and 11, among them tricarboxylic acids, hydroxyl dicarboxylic acids and oxodicarboxylic acids, being detected for the first time.

Quantification and partitioning coefficient estimations were provided, although, as no precaution was taken to avoid or correct artifacts on both gas and particulate phases compounds quantification, their relevance for atmospheric conclusions are limited here. Nevertheless, decoupling gas and particulate sampling, method allows testing a wide

AMTD
5, 1153–1231, 2012

range of possibilities to limit (e.g. denuder use) or correct (e.g. backup filter use) artifacts.

Furthermore, derivatisation protocols should be improved to extend the range of quantifiable species to tri-functionalised compounds. To improve the confidence in experimental determination of partitioning coefficients for tri-carbonyl compounds, observed in limonene ozonolysis particulate phase samples, it appears necessary to assess detection limits in the gas phase and to provide more relevant calibration curves for the particulate phase. Keto-di-acids and tri-acids are quantifiable in the gas phase and are detected in limonene ozonolysis particulate phase samples. An adjustment of the derivatisation protocol for the particulate phase, such as a small increase of the derivatisation temperature, seems to be able to provide relevant calibration curves.

In conclusion, the developed method allows to explore the chemical composition of the semi-volatile fraction of the oxygenated secondary organic matter and to assess its partitioning behaviour from mono to di-functionalised carbonyl, hydroxyl and organic acids species. Further improvement could enlarge the quantifiable species in both gas and particulate phases to tri-functionalized compounds. The method is applicable to both simulation chamber experiments under realistic humidity conditions and field campaigns.

Supplementary material related to this article is available online at: http://www.atmos-meas-tech-discuss.net/5/1153/2012/amtd-5-1153-2012-supplement.pdf.

Acknowledgements. The authors wish to thank the EuPhoRe group at CEAM, Valencia for their contribution to simulation chamber experiments. This work was supported by the EC within the I3 project "Integrating of European Simulation Chambers for Investigating Atmospheric Processes – II" (EUROCHAMP-2, contract no. 228335).

AMTD
5, 1153–1231, 2012

The publication of this article is financed by CNRS-INSU.

References

Arp, H. P. H., Schwarzenbach, R. P., and Goss, K. U.: Equilibrium sorption of gaseous organic chemicals to fiber filters used for aerosol studies, Atmos. Environ., 41, 8241–8252, doi:10.1016/j.atmosenv.2007.06.026, 2007.

Asher, W. E. and Pankow, J. F.: Vapor pressure prediction for alkenoic and aromatic organic compounds by a UNIFAC-based group contribution method, Atmos. Environ., 40, 3588–3600, doi:10.1016/j.atmosenv.2005.12.004, 2006.

Baltussen, E. B., Cramers, C. C., and Sandra, P. S.: Sorptive sample preparation – a review, Anal. Bioanal. Chem., 373, 3–22, 2002.

Barley, M. H. and McFiggans, G.: The critical assessment of vapour pressure estimation methods for use in modelling the formation of atmospheric organic aerosol, Atmos. Chem. Phys., 10, 749–767, doi:10.5194/acp-10-749-2010, 2010.

Beiner, K., Plewka, A., Haferkorn, S., Iinuma, Y., Engewald, W., and Herrmann, H.: Quantification of organic acids in particulate matter by coupling of thermally assisted hydrolysis and methylation with thermodesorption-gas chromatography-mass spectrometry, J. Chromatogr. A, 1216, 6642–6650, doi:10.1016/j.chroma.2009.07.054, 2009.

Bessagnet, B., Menut, L., Curci, G., Hodzic, A., Guillaume, B., Liousse, C., Moukhtar, S., Pun, B., Seigneur, C., and Schulz, M.: Regional modeling of carbonaceous aerosols over Europe-focus on secondary organic aerosols, J. Atmos. Chem., 61, 175–202, doi:10.1007/s10874-009-9129-2, 2008.

Blake, R. S., Whyte, C., Hughes, C. O., Ellis, A. M., and Monks, P. S.: Demonstration of proton-transfer reaction time-of-flight mass spectrometry for real-time analysis of trace volatile organic compounds, Anal. Chem., 76, 3841–3845, doi:10.1021/ac0498260, 2004.

AMTD
5, 1153–1231, 2012

Camredon, M., Aumont, B., Lee-Taylor, J., and Madronich, S.: The SOA/VOC/NO_x system: an explicit model of secondary organic aerosol formation, Atmos. Chem. Phys., 7, 5599–5610, doi:10.5194/acp-7-5599-2007, 2007.

Camredon, M., Hamilton, J. F., Alam, M. S., Wyche, K. P., Carr, T., White, I. R., Monks, P. S., Rickard, A. R., and Bloss, W. J.: Distribution of gaseous and particulate organic composition during dark α-pinene ozonolysis, Atmos. Chem. Phys., 10, 2893–2917, doi:10.5194/acp-10-2893-2010, 2010.

Canagaratna, M. R., Jayne, J. T., Jimenez, J. L., Allan, J. D., Alfarra, M. R., Zhang, Q., Onasch, T. B., Drewnick, F., Coe, H., Middlebrook, A., Delia, A., Williams, L. R., Trimborn, A. M., Northway, M. J., DeCarlo, P. F., Kolb, C. E., Davidovits, P., and Worsnop, D. R.: Chemical and microphysical characterization of ambient aerosols with the aerodyne aerosol mass spectrometer, Mass Spectrom. Rev., 26, 185–222, 2007.

Cancilla, D. A. and Que Hee, S. S.: O-(2,3,4,5,6-Pentafluorophenyl)methylhydroxylamine hydrochloride: a versatile reagent for the determination of carbonyl-containing compounds, J. Chromatogr. A, 627, 1–16, doi:10.1016/0021-9673(92)87181-7, 1992.

Cappa, C. D. and Jimenez, J. L.: Quantitative estimates of the volatility of ambient organic aerosol, Atmos. Chem. Phys., 10, 5409–5424, doi:10.5194/acp-10-5409-2010, 2010.

Carrasco, N., Doussin, J. F., O'Connor, M., Wenger, J. C., Picquet-Varrault, B., Durand-Jolibois, R., and Carlier, P.: Simulation chamber studies of the atmospheric oxidation of 2-methyl-3-buten-2-ol: Reaction with hydroxyl radicals and ozone under a variety of conditions, J. Atmos. Chem., 56, 33–55, doi:10.1007/s10874-006-9041-y, 2007.

Castells, P., Santos, F. J., and Galceran, M. T.: Development of a sequential supercritical fluid extraction method for the analysis of nitrated and oxygenated derivatives of polycyclic aromatic hydrocarbons in urban aerosols, J. Chromatogr. A, 1010, 141–151, doi:10.1016/S0021-9673(03)01121-X, 2003.

Chan, M. N., Chan, A. W. H., Chhabra, P. S., Surratt, J. D., and Seinfeld, J. H.: Modeling of secondary organic aerosol yields from laboratory chamber data, Atmos. Chem. Phys., 9, 5669–5680, doi:10.5194/acp-9-5669-2009, 2009.

Chan, M. N., Surratt, J. D., Claeys, M., Edgerton, E. S., Tanner, R. L., Shaw, S. L., Zheng, M., Knipping, E. M., Eddingsaas, N. C., Wennberg, P. O., and Seinfeld, J. H.: Characterization and quantification of isoprene-derived epoxydiols in ambient aerosol in the Southeastern United States, Environ. Sci. Technol., 44, 4590–4596, doi:10.1021/es100596b, 2010.

AMTD
5, 1153–1231, 2012

Chiappini, L., Perraudin, E., Durand-Jolibois, R., and Doussin, J. F.: Development of a supercritical fluid extraction-gas chromatography-mass spectrometry method for the identification of highly polar compounds in secondary organic aerosols formed from biogenic hydrocarbons in smog chamber experiments, Anal. Bioanal. Chem., 386, 1749–1759, doi:10.1007/s00216-006-0744-3, 2006.

Claeys, M., Graham, B., Vas, G., Wang, W., Vermeylen, R., Pashynska, V., Cafmeyer, J., Guyon, P., Andreae, M. O., Artaxo, P., and Maenhaut, W.: Formation of secondary organic aerosols through photooxidation of isoprene, Science, 303, 1173–1176, doi:10.1126/science.1092805, 2004.

Claeys, M., Szmigielski, R., Kourtchev, I., Van der Veken, P., Vermeylen, R., Maenhaut, W., Jaoui, M., Kleindienst, T. E., Lewandowski, M., Offenberg, J. H., and Edney, E. O.: Hydroxydicarboxylic acids: markers for secondary organic aerosol from the photooxidation of a-pinene, Environ. Sci. Technol., 41, 1628–1634, doi:10.1021/es0620181, 2007.

Claeys, M., Iinuma, Y., Szmigielski, R., Surratt, J. D., Blockhuys, F., Van Alsenoy, C., Boge, O., Sierau, B., Gomez-Gonzalez, Y., Vermeylen, R., Van der Veken, P., Shahgholi, M., Chan, A. W. H., Herrmann, H., Seinfeld, J. H., and Maenhaut, W.: Terpenylic acid and related compounds from the oxidation of α-pinene: implications for new particle formation and growth above forests, Environ. Sci. Technol., 43, 6976–6982, doi:10.1021/es9007596, 2009.

Clausen, P. A., Wilkins, C. K., Wolkoff, P., and Nielsen, G. D.: Chemical and biological evaluation of a reaction mixture of R-(+)-limonene/ozone: Formation of strong airway irritants, Environ. Int., 26, 511–522, doi:10.1016/S0160-4120(01)00035-6, 2001.

Coleman, B. K., Lunden, M. M., Destaillats, H., and Nazaroff, W. W.: Secondary organic aerosol from ozone-initiated reactions with terpene-rich household products, Atmos. Environ., 42, 8234–8245, doi:10.1016/j.atmosenv.2008.07.031, 2008.

de Gouw, J. and Warneke, C.: Measurements of volatile organic compounds in the earth's atmosphere using proton-transfer-reaction mass spectrometry, Mass Spectrom. Rev., 26, 223–257, 2007.

Docherty, K. S. and Ziemann, P. J.: Effects of stabilized Criegee intermediate and OH radical scavengers on aerosol formation from reactions of α-pinene with O_3, Aerosol Sci. Tech., 37, 877–891, doi:10.1080/02786820300930, 2003.

Donahue, N. M., Robinson, A. L., Stanier, C. O., and Pandis, S. N.: Coupled partitioning, dilution, and chemical aging of semivolatile organics, Environ. Sci. Technol., 40, 02635–02643, doi:10.1021/es052297c, 2006.

AMTD
5, 1153–1231, 2012

Donahue, N. M., Robinson, A. L., and Pandis, S. N.: Atmospheric organic particulate matter: From smoke to secondary organic aerosol, Atmos. Environ., 43, 94–106, doi:10.1016/j.atmosenv.2008.09.055, 2009.

Edney, E. O., Kleindienst, T. E., Jaoui, M., Lewandowski, M., Offenberg, J. H., Wang, W., and Claeys, M.: Formation of 2-methyl tetrols and 2-methylglyceric acid in secondary organic aerosol from laboratory irradiated isoprene/NOX/SO2/air mixtures and their detection in ambient $PM_{2.5}$ samples collected in the eastern United States, Atmos. Environ., 39, 5281–5289, doi:10.1016/j.atmosenv.2005.05.031, 2005.

Farina, S. C., Adams, P. J., and Pandis, S. N.: Modeling global secondary organic aerosol formation and processing with the volatility basis set: Implications for anthropogenic secondary organic aerosol, J. Geophys. Res.-Atmos., 115, D09202, doi:10.1029/2009jd013046, 2010.

Forester, C. D. and Wells, J. R.: Yields of Carbonyl Products from Gas-Phase Reactions of Fragrance Compounds with OH Radical and Ozone, Environ. Sci. Technol., 43, 3561–3568, doi:10.1021/es803465v, 2009.

Forstner, H. J. L., Flagan, R. C., and Seinfeld, J. H.: Molecular speciation of secondary organic aerosol from photooxidation of the higher alkenes: 1-octene and 1-decene, Atmos. Environ., 31, 1953–1964, doi:10.1016/s1352-2310(96)00356-1, 1997.

Goldstein, A. H., Worton, D. R., Williams, B. J., Hering, S. V., Kreisberg, N. M., Panic, O., and Górecki, T.: Thermal desorption comprehensive two-dimensional gas chromatography for in-situ measurements of organic aerosols, J. Chromatogr. A, 1186, 340–347, doi:10.1016/j.chroma.2007.09.094, 2008.

Gonzalez-Flesca, N. and Frezier, A.: A new laboratory test chamber for the determination of diffusive sampler uptake rates, Atmos. Environ., 39, 4049–4056, doi:10.1016/j.atmosenv.2005.03.025, 2005.

Graber, E. R. and Rudich, Y.: Atmospheric HULIS: How humic-like are they? A comprehensive and critical review, Atmos. Chem. Phys., 6, 729–753, doi:10.5194/acp-6-729-2006, 2006.

Grieshop, A. P., Miracolo, M. A., Donahue, N. M., and Robinson, A. L.: Constraining the volatility distribution and gas-particle partitioning of combustion aerosols using isothermal dilution and thermodenuder Measurements, Environ. Sci. Technol., 43, 4750–4756, doi:10.1021/es8032378, 2009.

Griffin, R. J., Cocker III, D. R., Seinfeld, J. H., and Dabdub, D.: Estimate of global atmospheric organic aerosol from oxidation of biogenic hydrocarbons, Geophys. Res. Lett., 26, 2721–2724, doi:10.1029/1999GL900476, 1999.

AMTD
5, 1153–1231, 2012

Guenther, A., Hewitt, C. N., Erickson, D., Fall, R., Geron, C., Graedel, T., Harley, P., Klinger, L., Lerdau, M., McKay, W. A., Pierce, T., Scholes, B., Steinbrecher, R., Tallamraju, R., Taylor, J., and Zimmerman, P.: A global-model of natural volatile organic-compound emissions, J. Geophys. Res.-Atmos., 100, 8873–8892, doi:10.1029/94jd02950, 1995.

Hallquist, M., Wenger, J. C., Baltensperger, U., Rudich, Y., Simpson, D., Claeys, M., Dommen, J., Donahue, N. M., George, C., Goldstein, A. H., Hamilton, J. F., Herrmann, H., Hoffmann, T., Iinuma, Y., Jang, M., Jenkin, M. E., Jimenez, J. L., Kiendler-Scharr, A., Maenhaut, W., McFiggans, G., Mentel, Th. F., Monod, A., Prévôt, A. S. H., Seinfeld, J. H., Surratt, J. D., Szmigielski, R., and Wildt, J.: The formation, properties and impact of secondary organic aerosol: current and emerging issues, Atmos. Chem. Phys., 9, 5155–5236, doi:10.5194/acp-9-5155-2009, 2009.

Hamilton, J. F., Webb, P. J., Lewis, A. C., and Reviejo, M. M.: Quantifying small molecules in secondary organic aerosol formed during the photo-oxidation of toluene with hydroxyl radicals, Atmos. Environ., 39, 7263–7275, doi:10.1016/j.atmosenv.2005.09.006, 2005.

Hamilton, J. F., Rami Alfarra, M., Wyche, K. P., Ward, M. W., Lewis, A. C., McFiggans, G. B., Good, N., Monks, P. S., Carr, T., White, I. R., and Purvis, R. M.: Investigating the use of secondary organic aerosol as seed particles in simulation chamber experiments, Atmos. Chem. Phys., 11, 5917–5929, doi:10.5194/acp-11-5917-2011, 2011.

Hansen, K. J., Nansen, B. N., Cravens, E., and Sievers, R. E.: Supercritical-fluid extraction gas-chromatographic analysis of organic-compounds in atmospheric aerosols, Anal. Chem., 67, 3541–3549, doi:10.1021/ac00115a025, 1995.

Harper, M.: Evaluation of solid sorbent sampling methods by breakthrough volume studies, Ann. Occup. Hyg., 37, 65–88, doi:10.1093/annhyg/37.1.65, 1993.

Hays, M. D. and Lavrich, R. J.: Developments in direct thermal extraction gas chromatography-mass spectrometry of fine aerosols, TrAC Trend Anal. Chem., 26, 88–102, 2007.

Healy, R. M., Wenger, J. C., Metzger, A., Duplissy, J., Kalberer, M., and Dommen, J.: Gas/particle partitioning of carbonyls in the photooxidation of isoprene and 1,3,5-trimethylbenzene, Atmos. Chem. Phys., 8, 3215–3230, doi:10.5194/acp-8-3215-2008, 2008.

Healy, R. M., Temime, B., Kuprovskyte, K., and Wenger, J. C.: Effect of relative humidity on gas/particle partitioning and aerosol mass yield in the photooxidation of *p*-xylene, Environ. Sci. Technol., 43, 1884–1889, doi:10.1021/es802404z, 2009.

Ho, S. S. H. and Yu, J. Z.: Feasibility of collection and analysis of airborne carbonyls by on-sorbent derivatization and thermal desorption, Anal. Chem., 74, 1232–1240,

AMTD
5, 1153–1231, 2012

doi:10.1021/ac015708q, 2002.
Ho, S. S. H. and Yu, J. Z.: Determination of airborne carbonyls: Comparison of a thermal desorption/GC method with the standard DNPH/HPLC method, Environ. Sci. Technol., 38, 862–870, doi:10.1021/es034784w, 2004.
IPCC: Fourth Assessment Report: Climate Change 2007, The Physical Science Basis, Cambridge University Press, Cambridge, UK and New York, NY, USA, 2007.
Isaacman, G., Worton, D. R., Kreisberg, N. M., Hennigan, C. J., Teng, A. P., Hering, S. V., Robinson, A. L., Donahue, N. M., and Goldstein, A. H.: Understanding evolution of product composition and volatility distribution through in-situ GC × GC analysis: a case study of longifolene ozonolysis, Atmos. Chem. Phys., 11, 5335–5346, doi:10.5194/acp-11-5335-2011, 2011.
Jakober, C. A., Robert, M. A., Riddle, S. G., Destaillats, H., Charles, M. J., Green, P. G., and Kleeman, M. J.: Carbonyl emissions from gasoline and diesel motor vehicles, Environ. Sci. Technol., 42, 4697–4703, doi:10.1021/es7029174, 2008.
Jaoui, M. and Kamens, R. M.: Gaseous and particulate oxidation products analysis of a mixture of α-pinene + β-pinene/O_3/Air in the absence of light and α-pinene + β-pinene/NO_x/Air in the presence of natural sunlight, J. Atmos. Chem., 44, 259–297, 2003.
Jaoui, M., Leungsakul, S., and Kamens, R. M.: Gas and particle products distribution from the reaction of β-caryophyllene with ozone, J. Atmos. Chem., 45, 261–287, 2003.
Jaoui, M., Corse, E., Kleindienst, T. E., Offenberg, J. H., Lewandowski, M., and Edney, E. O.: Analysis of secondary organic aerosol compounds from the photooxidation of d-limonene in the presence of NOX and their detection in ambient $PM_{2.5}$, Environ. Sci. Technol., 40, 3819–3828, doi:10.1021/es052566z, 2006.
Jardine, K., Serrano, A. Y., Arneth, A., Abrell, L., Jardine, A., van Haren, J., Artaxo, P., Rizzo, L. V., Ishida, F. Y., Karl, T., Kesselmeier, J., Saleska, S., and Huxman, T.: Within-canopy sesquiterpene ozonolysis in Amazonia, J. Geophys. Res.-Atmos., 116, D19301, doi:10.1029/2011jd016243, 2011.
Jenkin, M. E.: Modelling the formation and composition of secondary organic aerosol from α- and β-pinene ozonolysis using MCM v3, Atmos. Chem. Phys., 4, 1741–1757, doi:10.5194/acp-4-1741-2004, 2004.
Jenkin, M. E., Saunders, S. M., and Pilling, M. J.: The tropospheric degradation of volatile organic compounds: a protocol for mechanism development, Atmos. Environ., 31, 81–104, doi:10.1016/S1352-2310(96)00105-7, 1997.

AMTD
5, 1153–1231, 2012

Jonsson, A. M., Hallquist, M., and Ljungstrom, E.: Influence of OH scavenger on the water effect on secondary organic aerosol formation from ozonolysis of limonene, delta(3)-carene, and alpha-pinene, Environ. Sci. Technol., 42, 5938–5944, doi:10.1021/es702508y, 2008.
Kalberer, M., Yu, J., Cocker, D. R., Flagan, R. C., and Seinfeld, J. H.: Aerosol formation in the cyclohexene-ozone system, Environ. Sci. Technol., 34, 4894–4901, doi:10.1021/es001180f, 2000.
Kanakidou, M., Seinfeld, J. H., Pandis, S. N., Barnes, I., Dentener, F. J., Facchini, M. C., Van Dingenen, R., Ervens, B., Nenes, A., Nielsen, C. J., Swietlicki, E., Putaud, J. P., Balkanski, Y., Fuzzi, S., Horth, J., Moortgat, G. K., Winterhalter, R., Myhre, C. E. L., Tsigaridis, K., Vignati, E., Stephanou, E. G., and Wilson, J.: Organic aerosol and global climate modelling: a review, Atmos. Chem. Phys., 5, 1053–1123, doi:10.5194/acp-5-1053-2005, 2005.
Kitanovski, Z., Grgic, I., and Veber, M.: Characterization of carboxylic acids in atmospheric aerosols using hydrophilic interaction liquid chromatography tandem mass spectrometry, J. Chromatogr. A, 1218, 4417–4425, doi:10.1016/j.chroma.2011.05.020, 2011.
Kleindienst, T. E., Conver, T. S., McIver, C. D., and Edney, E. O.: Determination of secondary organic aerosol products from the photooxidation of toluene and their implications in ambient $PM_{2.5}$, J. Atmos. Chem., 47, 79–100, 2004.
Kroll, J. H., Ng, N. L., Murphy, S. M., Flagan, R. C., and Seinfeld, J. H.: Secondary organic aerosol formation from isoprene photooxidation, Environ. Sci. Technol., 40, 1869–1877, doi:10.1021/es0524301, 2006.
Kroll, J. H., Chan, A. W. H., Ng, N. L., Flagan, R. C., and Seinfeld, J. H.: Reactions of semivolatile organics and their effects on secondary organic aerosol formation, Environ. Sci. Technol., 41, 3545–3550, doi:10.1021/es062059x, 2007.
Langer, S., Moldanová, J., Arrhenius, K., Ljungström, E., and Ekberg, L.: Ultrafine particles produced by ozone/limonene reactions in indoor air under low/closed ventilation conditions, Atmos. Environ., 42, 4149–4159, doi:10.1016/j.atmosenv.2008.01.034, 2008.
Lazaridis, M.: Gas-particle partitioning of organic compounds in the atmosphere, J. Aerosol Sci., 30, 1165–1170, doi:10.1016/S0021-8502(98)00788-5, 1999.
Lee, B.-H., Pierce, J. R., Engelhart, G. J., and Pandis, S. N.: Volatility of secondary organic aerosol from the ozonolysis of monoterpenes, Atmos. Environ., 45, 2443–2452, doi:10.1016/j.atmosenv.2011.02.004, 2011.
Lee, S., Jang, M., and Kamens, R. M.: SOA formation from the photooxidation of α-pinene in the presence of freshly emitted diesel soot exhaust, Atmos. Environ., 38, 2597–2605,

AMTD
5, 1153–1231, 2012

doi:10.1016/j.atmosenv.2003.12.041, 2004.
Legrand, M., Preunkert, S., Galy-Lacaux, C., Liousse, C., and Wagenbach, D.: Atmospheric year-round records of dicarboxylic acids and sulfate at three French sites located between 630 and 4360 m elevation, J. Geophys. Res.-Atmos., 110, D13302, doi:10.1029/2004jd005515, 2005.
Leungsakul, S., Jaoui, M., and Kamens, R. M.: Kinetic mechanism for predicting secondary organic aerosol formation from the reaction of d-limonene with ozone, Environ. Sci. Technol., 39, 9583–9594, doi:10.1021/es0492687, 2005a.
Leungsakul, S., Jeffries, H. E., and Kamens, R. M.: A kinetic mechanism for predicting secondary aerosol formation from the reactions of *d*-limonene in the presence of oxides of nitrogen and natural sunlight, Atmos. Environ., 39, 7063–7082, doi:10.1016/j.atmosenv.2005.08.024, 2005b.
Li, J., Feng, Y. L., Xie, C. J., Huang, J., Yu, J. Z., Feng, J. L., Sheng, G. Y., Fu, J. M., and Wu, M. H.: Determination of gaseous carbonyl compounds by their pentafluorophenyl hydrazones with gas chromatography/mass spectrometry, Anal. Chim. Acta, 635, 84–93, doi:10.1016/j.aca.2008.12.041, 2009.
Li, Y.-C. and Yu, J. Z.: Simultaneous determination of mono- and dicarboxylic acids, ω-oxocarboxylic acids, midchain ketocarboxylic acids, and aldehydes in atmospheric aerosol samples, Environ. Sci. Technol., 39, 7616–7624, doi:10.1021/es050896d, 2005.
Liggio, J. and McLaren, R.: An optimized method for the determination of volatile and semivolatile aldehydes and ketones in ambient particulate matter, Int. J. Environ. Anal. Chem., 83, 819–835, doi:10.1080/03067310310001597653, 2003.
Loedwyckx, P. and Vansant, E. F.: The influence of humidity on the overall mass transfer coefficient of the Wheeler-Jonas equation, Am. Ind. Hyg. Assoc. J., 61, 461–468, 2000.
Martin, N. A., Marlow, D. J., Henderson, M. H., Goody, B. A., and Quincey, P. G.: Studies using the sorbent Carbopack *X* for measuring environmental benzene with Perkinâ"Elmer-type pumped and diffusive samplers, Atmos. Environ., 37, 871–879, doi:10.1016/S1352-2310(02)01000-2, 2003.
Matsunaga, S., Mochida, M., and Kawamura, K.: High abundance of gaseous and particulate 4-oxopentanal in the forestal atmosphere, Chemosphere, 55, 1143–1147, doi:10.1016/j.chemosphere.2003.10.004, 2004.

AMTD
5, 1153–1231, 2012

Monks, P. S., Granier, C., Fuzzi, S., Stohl, A., Williams, M. L., Akimoto, H., Amann, M., Baklanov, A., Baltensperger, U., Bey, I., Blake, N., Blake, R. S., Carslaw, K., Cooper, O. R., Dentener, F., Fowler, D., Fragkou, E., Frost, G. J., Generoso, S., Ginoux, P., Grewe, V., Guenther, A., Hansson, H. C., Henne, S., Hjorth, J., Hofzumahaus, A., Huntrieser, H., Isaksen, I. S. A., Jenkin, M. E., Kaiser, J., Kanakidou, M., Klimont, Z., Kulmala, M., Laj, P., Lawrence, M. G., Lee, J. D., Liousse, C., Maione, M., McFiggans, G., Metzger, A., Mieville, A., Moussiopoulos, N., Orlando, J. J., O'Dowd, C. D., Palmer, P. I., Parrish, D. D., Petzold, A., Platt, U., Pöschl, U., Prévôt, A. S. H., Reeves, C. E., Reimann, S., Rudich, Y., Sellegri, K., Steinbrecher, R., Simpson, D., ten Brink, H., Theloke, J., van der Werf, G. R., Vautard, R., Vestreng, V., Vlachokostas, C., and von Glasow, R.: Atmospheric composition change – global and regional air quality, Atmos. Environ., 43, 5268–5350, doi:10.1016/j.atmosenv.2009.08.021, 2009.

Müller, K., Haferkorn, S., Grabmer, W., Wisthaler, A., Hansel, A., Kreuzwieser, J., Cojocariu, C., Rennenberg, H., and Herrmann, H.: Biogenic carbonyl compounds within and above a coniferous forest in Germany, Atmos. Environ., 40, Supplement 1, 81–91, doi:10.1016/j.atmosenv.2005.10.070, 2006.

Myrdal, P. B. and Yalkowsky, S. H.: Estimating pure component vapor pressures of complex organic molecules, Ind. Eng. Chem. Res., 36, 2494–2499, doi:10.1021/ie950242l, 1997.

Nannoolal, Y., Rarey, J. R., and Ramjugernath, D.: Estimation of pure component properties: Part 3, Estimation of the vapor pressure of non-electrolyte organic compounds via group contributions and group interactions, Fluid Phase Equilibr., 269, 117–133, doi:10.1016/j.fluid.2008.04.020, 2008.

Nolte, C. G., Schauer, J. J., Cass, G. R., and Simoneit, B. R. T.: Highly polar organic compounds present in wood smoke and in the ambient atmosphere, Environ. Sci. Technol., 35, 1912–1919, doi:10.1021/es001420r, 2001.

Northcross, A. L. and Jang, M.: Heterogeneous SOA yield from ozonolysis of monoterpenes in the presence of inorganic acid, Atmos. Environ., 41, 1483–1493, doi:10.1016/j.atmosenv.2006.10.009, 2007.

Odum, J. R., Hoffmann, T., Bowman, F., Collins, D., Flagan, R. C., and Seinfeld, J. H.: Gas/Particle Partitioning and Secondary Organic Aerosol Yields, Environ. Sci. Technol., 30, 2580–2585, 1996.

Orasche, J., Schnelle-Kreis, J., Abbaszade, G., and Zimmermann, R.: Technical Note: In-situ derivatization thermal desorption GC-TOFMS for direct analysis of particle-bound non-polar and polar organic species, Atmos. Chem. Phys., 11, 8977–8993, doi:10.5194/acp-11-8977-

AMTD
5, 1153–1231, 2012

2011, 2011.
Ortiz, R., Enya, K., Sekiguchi, K., and Sakamoto, K.: Experimental testing of an annular denuder and filter system to measure gas-particle partitioning of semivolatile bifunctional carbonyls in the atmosphere, Atmos. Environ., 43, 382–388, doi:10.1016/j.atmosenv.2008.09.074, 2009.
Ortiz, R., Enya, K., and Sakamoto, K.: Experimental Determination of the Partition Coefficient for Bifunctional Carbonyls in the Atmosphere and in Smog Chamber, in: Nato-Chal. M., NATO Science for Peace and Security Series B-Physics and Biophysics, 265–269, 2010.
Pacolay, B. D., Ham, J. E., Slaven, J. E., and Wells, J. R.: Feasibility of detection and quantification of gas-phase carbonyls in indoor environments using PFBHA derivatization and solid-phase microextraction (SPME), J. Environ. Monitor., 10, 853–860, doi:10.1039/b801926f, 2008.
Pankow, J. F.: An absorption model of gas/particle partitioning of organic compounds in the atmosphere, Atmos. Environ., 28, 185–188, doi:10.1016/1352-2310(94)90093-0, 1994.
Pankow, J. F.: On the ability of the gas/particle partitioning constant Kp to consider the effects of mean MW and the presence of high MW compounds, Atmos. Environ., 45, 1213–1216, doi:10.1016/j.atmosenv.2010.11.041, 2011.
Pankow, J. F. and Asher, W. E.: SIMPOL.1: a simple group contribution method for predicting vapor pressures and enthalpies of vaporization of multifunctional organic compounds, Atmos. Chem. Phys., 8, 2773–2796, doi:10.5194/acp-8-2773-2008, 2008.
Parikh, H. M., Carlton, A. G., Vizuete, W., and Kamens, R. M.: Modeling secondary organic aerosol using a dynamic partitioning approach incorporating particle aqueous-phase chemistry, Atmos. Environ., 45, 1126–1137, doi:10.1016/j.atmosenv.2010.11.027, 2011.
Pietrogrande, M. C. and Bacco, D.: GC-MS analysis of water-soluble organics in atmospheric aerosol: Response surface methodology for optimizing silyl-derivatization for simultaneous analysis of carboxylic acids and sugars, Anal. Chim. Acta, 689, 257–264, doi:10.1016/j.aca.2011.01.047, 2011.
Pietrogrande, M., Bacco, D., and Mercuriali, M.: GC-MS analysis of low-molecular-weight dicarboxylic acids in atmospheric aerosol: comparison between silylation and esterification derivatization procedures, Anal. Bioanal. Chem., 396, 877–885, 2010.
Pol, J., Hohnova, B., Jussila, M., and Hyotylainen, T.: Comprehensive two-dimensional liquid chromatography-time-of-flight mass spectrometry in the analysis of acidic compounds in atmospheric aerosols, J. Chromatogr. A, 1130, 64–71, doi:10.1016/j.chroma.2006.04.050,

AMTD
5, 1153–1231, 2012

2006.
Prather, K. A., Hatch, C. D., and Grassian, V. H.: Analysis of Atmospheric Aerosols, in: Annu. Rev. Anal. Chem., Annual Review of Analytical Chemistry, Annual Reviews, Palo Alto, 485–514, 2008.
Rudich, Y.: Laboratory Perspectives on the Chemical Transformations of Organic Matter in Atmospheric Particles, Chem. Rev., 103, 5097–5124, doi:10.1021/cr020508f, 2003.
Rudich, Y., Donahue, N. M., and Mentel, T. F.: Aging of organic aerosol: Bridging the gap between laboratory and field studies, Annu. Rev. Phys. Chem., 58, 321–352, doi:10.1146/annurev.physchem.58.032806.104432, 2007.
Saathoff, H., Naumann, K.-H., Möhler, O., Jonsson, Å. M., Hallquist, M., Kiendler-Scharr, A., Mentel, Th. F., Tillmann, R., and Schurath, U.: Temperature dependence of yields of secondary organic aerosols from the ozonolysis of α-pinene and limonene, Atmos. Chem. Phys., 9, 1551–1577, doi:10.5194/acp-9-1551-2009, 2009.
Sarwar, G. and Corsi, R.: The effects of ozone/limonene reactions on indoor secondary organic aerosols, Atmos. Environ., 41, 959–973, doi:10.1016/j.atmosenv.2006.09.032, 2007.
Sato, K., Takami, A., Isozaki, T., Hikida, T., Shimono, A., and Imamura, T.: Mass spectrometric study of secondary organic aerosol formed from the photo-oxidation of aromatic hydrocarbons, Atmos. Environ., 44, 1080–1087, doi:10.1016/j.atmosenv.2009.12.013, 2010.
Saunders, S. M., Jenkin, M. E., Derwent, R. G., and Pilling, M. J.: Protocol for the development of the Master Chemical Mechanism, MCM v3 (Part A): tropospheric degradation of non-aromatic volatile organic compounds, Atmos. Chem. Phys., 3, 161–180, doi:10.5194/acp-3-161-2003, 2003.
Seinfeld, J. H. and Pankow, J. F.: Organic atmospheric particulate material, Annu. Rev. Phys. Chem., 54, 121–140, doi:10.1146/annurev.physchem.54.011002.103756, 2003.
Sheesley, R. J., DeMinter, J. T., Meiritz, M., Snyder, D. C., and Schauer, J. J.: Temporal trends in motor vehicle and secondary organic tracers using in situ methylation thermal desorption GC-MS, Environ. Sci. Technol., 44, 9398–9404, doi:10.1021/es102301t, 2010.
Shimmo, M., Jäntti, J., Aalto, P., Hartonen, K., Hyötyläinen, T., Kulmala, M., and Riekkola, M.-L.: Characterisation of organic compounds in aerosol particles from a Finnish forest by on-line coupled supercritical fluid extraction-liquid chromatography-gas chromatography-mass spectrometry, Anal. Bioanal. Chem., 378, 1982–1990, 2004.

AMTD
5, 1153–1231, 2012

Singer, B. C., Destaillats, H., Hodgson, A. T., and Nazaroff, W. W.: Cleaning products and air fresheners: emissions and resulting concentrations of glycol ethers and terpenoids, Indoor Air, 16, 179–191, 2006.
Sinha, V., Williams, J., Lelieveld, J., Ruuskanen, T. M., Kajos, M. K., Patokoski, J., Hellen, H., Hakola, H., Mogensen, D., Boy, M., Rinne, J., and Kulmala, M.: OH reactivity measurements within a boreal forest: evidence for unknown reactive emissions, Environ. Sci. Technol., 44, 6614–6620, doi:10.1021/es101780b, 2010.
Sullivan, R. C. and Prather, K. A.: Recent advances in our understanding of atmospheric chemistry and climate made possible by on-line aerosol analysis instrumentation, Anal. Chem., 77, 3861–3886, doi:10.1021/ac050716i, 2005.
Sun, J. and Ariya, P. A.: Atmospheric organic and bio-aerosols as cloud condensation nuclei (CCN): A review, Atmos. Environ., 40, 795–820, doi:10.1016/j.atmosenv.2005.05.052, 2006.
Sun, T., Wang, Y., Zhang, C., Sun, X., and Wang, W.: The chemical mechanism of the limonene ozonolysis reaction in the SOA formation: A quantum chemistry and direct dynamic study, Atmos. Environ., 45, 1725–1731, doi:10.1016/j.atmosenv.2010.12.054, 2011.
Szmigielski, R., Surratt, J. D., Vermeylen, R., Szmigielska, K., Kroll, J. H., Ng, N. L., Murphy, S. M., Sorooshian, A., Seinfeld, J. H., and Claeys, M.: Characterization of 2-methylglyceric acid oligomers in secondary organic aerosol formed from the photooxidation of isoprene using trimethylsilylation and gas chromatography/ion trap mass spectrometry, J. Mass Spectrom., 42, 101–116, 2007.
Temime, B., Healy, R. M., and Wenger, J. C.: A denuder-filter sampling technique for the detection of gas and particle phase carhonyl compounds, Environ. Sci. Technol., 41, 6514–6520, doi:10.1021/es070802v, 2007.
Tsimpidi, A. P., Karydis, V. A., Zavala, M., Lei, W., Molina, L., Ulbrich, I. M., Jimenez, J. L., and Pandis, S. N.: Evaluation of the volatility basis-set approach for the simulation of organic aerosol formation in the Mexico City metropolitan area, Atmos. Chem. Phys., 10, 525–546, doi:10.5194/acp-10-525-2010, 2010.
Valorso, R., Aumont, B., Camredon, M., Raventos-Duran, T., Mouchel-Vallon, C., Ng, N. L., Seinfeld, J. H., Lee-Taylor, J., and Madronich, S.: Explicit modelling of SOA formation from a-pinene photooxidation: sensitivity to vapour pressure estimation, Atmos. Chem. Phys., 11, 6895–6910, doi:10.5194/acp-11-6895-2011, 2011.

AMTD
5, 1153–1231, 2012

Vivanco, M. G., Santiago, M., Martinez-Tarifa, A., Borras, E., Rodenas, M., Garcia-Diego, C., and Sanchez, M.: SOA formation in a photoreactor from a mixture of organic gases and HONO for different experimental conditions, Atmos. Environ., 45, 708–715, doi:10.1016/j.atmosenv.2010.09.059, 2011.

Volckens, J. and Leith, D.: Effects of sampling bias on gas-particle partitioning of semi-volatile compounds, Atmos. Environ., 37, 3385–3393, doi:10.1016/S1352-2310(03)00356-X, 2003.

Volkamer, R., Martini, F. S., Molina, L. T., Salcedo, D., Jimenez, J. L., and Molina, M. J.: A missing sink for gas-phase glyoxal in Mexico City: Formation of secondary organic aerosol, Geophys. Res. Lett., 34, L19807, doi:10.1029/2007gl030752, 2007.

Walser, M. L., Park, J., Gomez, A. L., Russell, A. R., and Nizkorodov, S. A.: Photochemical aging of secondary organic aerosol particles generated from the oxidation of d-limonene, J. Phys. Chem. A, 111, 1907–1913, doi:10.1021/jp066293l, 2007.

Wang, J., Doussin, J. F., Perrier, S., Perraudin, E., Katrib, Y., Pangui, E., and Picquet-Varrault, B.: Design of a new multi-phase experimental simulation chamber for atmospheric photosmog, aerosol and cloud chemistry research, Atmos. Meas. Tech., 4, 2465–2494, doi:10.5194/amt-4-2465-2011, 2011.

Warscheid, B., Kuckelmann, U., and Hoffmann, T.: Direct quantitative analysis of organic compounds in the gas and particle phase using a modified atmospheric pressure chemical ionization source in combination with ion trap mass spectrometry, Anal. Chem., 75, 1410–1417, doi:10.1021/ac025788d, 2003.

Wedel, A., Müller, K.-P., Ratte, M., and Rudolph, J.: Measurements of Volatile Organic Compounds (VOC) during POPCORN 1994: Applying a new on-line GC-MS technique, J. Atmos. Chem., 31, 73–103, 1998.

Williams, B. J., Goldstein, A. H., Kreisberg, N. M., and Hering, S. V.: An In-Situ Instrument for Speciated Organic Composition of Atmospheric Aerosols: Thermal Desorption Aerosol GC/MS-FID (TAG), Aerosol Sci. Tech., 40, 627–638, doi:10.1080/02786820600754631, 2006.

Woo, K.-L. and Kim, J.-I.: New hydrolysis method for extremely small amount of lipids and capillary gas chromatographic analysis as N(O)-tert.-butyldimethylsilyl fatty acid derivatives compared with methyl ester derivatives, J. Chromatogr. A, 862, 199–208, doi:10.1016/S0021-9673(99)00934-6, 1999.

Wu, L. J. and Hee, S. S. Q.: A solid sorbent personal air sampling method for aldehydes, Am. Ind. Hyg. Assoc. J., 56, 362–367, doi:10.1080/15428119591016980, 1995.

AMTD
5, 1153–1231, 2012

Wu, T., Wang, X., Li, D., Sheng, G., and Fu, J.: Determination of trace volatile fatty acids in ambient air by capillary gas chromatography-mass spectrometry in SIM mode, Int. J. Environ. Anal. Chem., 88, 1107–1115, doi:10.1080/03067310802447034, 2008.

Xu, X., Stee, L. L. P., Williams, J, Beens, J., Adahchour, M., Vreuls, R. J. J., Brinkman, U. A., and Lelieveld, J.: Comprehensive two-dimensional gas chromatography (GC × GC) measurements of volatile organic compounds in the atmosphere, Atmos. Chem. Phys., 3, 665–682, doi:10.5194/acp-3-665-2003, 2003.

Yasmeen, F., Szmigielski, R., Vermeylen, R., Gómez-González, Y., Surratt, J. D., Chan, A. W. H., Seinfeld, J. H., Maenhaut, W., and Claeys, M.: Mass spectrometric characterization of isomeric terpenoic acids from the oxidation of α-pinene, β-pinene, d-limonene, and Δ3-carene in fine forest aerosol, J. Mass Spectrom., 46, 425–442, 2011.

Yu, J., Cocker, D. R., Griffin, R. J., Flagan, R. C., and Seinfeld, J. H.: Gas-phase ozone oxidation of monoterpenes: gaseous and particulate products, J. Atmos. Chem., 34, 207–258, 1999.

Zhang, Q., Jimenez, J. L., Canagaratna, M. R., Ulbrich, I. M., Ng, N. L., Worsnop, D. R., and Sun, Y.: Understanding atmospheric organic aerosols via factor analysis of aerosol mass spectrometry: a review, Anal. Bioanal. Chem., 401, 3045–3067, 2011.

AMTD
5, 1153–1231, 2012

Table 1. Calibration curves slopes, linearities and detection limits for gaseous carbonyl compounds trapped on PFBHA coated Tenax TA tubes.

Standard Compound	Extracted ion (m/z)	Calibration curve slope	Y-intercept	Linearity (R^2)	Detection limits		
					ng tube^{-1}	ng m^{-3}*	ppt*
Aldehydes							
Pentanal	181	$(6.8 \pm 0.2) \times 10^5$		0.9993	0.3	25	7.1
2-EthylButanal	239	$(1.11 \pm 0.03) \times 10^5$		0.9995	0.1	9	2.2
3-Methyl-2-Butenal	264	$(1.03 \pm 0.01) \times 10^5$		0.9999	0.07	6	1.8
Heptanal	181	$(5.9 \pm 0.1) \times 10^5$		0.9998	0.3	25	5.4
Ethyl 3-Methyl-4-oxocrotonate	140	$(1.97 \pm 0.02) \times 10^4$		0.9999	0.3	25	4.3
Citronellal	168	$(7.01 \pm 0.05) \times 10^4$	$(1.8 \pm 0.7) \times 10^5$	0.9997	3	250	40
Citral	69	$(1.88 \pm 0.03) \times 10^5$	$(1.0 \pm 0.5) \times 10^6$	0.9990	6	500	80
Perillaldehyde	164	$(6.92 \pm 0.06) \times 10^4$		0.9998	0.1	9	1.5
Glutaraldehyde	181	$(9.7 \pm 0.6) \times 10^5$		0.9952	0.1	9	2.2
Ketones							
3-Penten-2-one	264	$(3.21 \pm 0.07) \times 10^4$		0.9997	0.1	9	2.6
3-Hydroxy-3-methyl-2-butanone	181	$(1.1 \pm 0.2) \times 10^5$		0.9883	1	84	20
2-Hexanone	181	$(7.5 \pm 0.6) \times 10^4$		0.9962	2	167	41
4-Heptanone	128	$(1.08 \pm 0.05) \times 10^4$		0.9988	0.9	75	16
5-Hydroxy-2-pentanone	279	$(1.89 \pm 0.04) \times 10^3$		0.9992	2	167	40
(+)-Dihydrocarvone	93	$(3.91 \pm 0.08) \times 10^4$		0.9997	1	84	14
Carvone	304	$(4.0 \pm 0.4) \times 10^4$		0.9914	0.09	8	1.3
DiMethyl Glyoxal	476	$(6.6 \pm 0.4) \times 10^2$		0.9970	7.0	584	166
3-Methyl-2,4-pentanedione	181	$(4.2 \pm 0.2) \times 10^5$		0.9983	0.4	34	7.3
Keto-aldehydes							
Methyl Glyoxal	181	$(1.7 \pm 0.4) \times 10^6$		0.9742	0.05	5	1.7
4-OxoPentanal	181	$(6.7 \pm 0.2) \times 10^5$		0.9997	0.02	2	0.5

* Given for a sampling volume of 12 l.

AMTD
5, 1153–1231, 2012

Table 2. Breakthrough data for a series of hydroxyl and carboxyl compounds identified from an isoprene photo-oxidation experiment vs. compound nature, molar mass, derivatisable functions number and retention times (indicatives).

Identified compound	Compound nature (carbon number and functions)	Molecular Weight ($g\,mol^{-1}$) (MTBSTFA derivatisable functions number)	Tr (min)	Breakthrough (%) (back-up tube area/ sample area)
Methacrylic acid	C4 mono acid	86 (1)	11.87	6
Crotonic acid	C4 mono acid	86 (1)	12.80	25
Valeric acid	C5 mono acid	102 (1)	13.36	3
3-EthylButyric acid	C6 mono acid	116 (1)	13.75	21
3-MethylPentanoic acid	C6 mono acid	116 (1)	14.68	52
Levulinic acid	C5 keto mono acid	116 (1)	15.58	<1
Heptanoic acid	C7 mono acid	130 (1)	15.99	0
1-MethylCyclohexaneCarboxylic acid*	C8 mono acid	142 (1)	16.10	0
Glycolic acid	C2 hydroxy acid	76 (2)	16.37	<1
2-HydroxyPropanoic acid	C3 hydroxy acid	90 (2)	17.25	<1
Oxalic acid	C2 di acid	90 (2)	17.92	<1
Maleic acid	C4 di acid	116 (2)	20.25	0
Succinic acid	C4 di acid	118 (2)	20.41	<1
Glutaric acid	C5 di acid	132 (2)	21.45	0
Glycerol	C3 tri alcohol	92 (3)	21.59	0
2,3-DihydroxyPropanoic acid	C3 di hydroxy mono acid	106 (3)	22.34	0
Adipic acid	C6 di acid	146 (2)	22.56	0
Suberic acid	C8 di acid	174 (2)	24.48	0
2-HydroxyPentanedioic acid	C5 hydroxy di acid	148 (3)	31.23	0

* Identified from a limonene ozonolysis experiment (see Sect. 4).

AMTD
5, 1153–1231, 2012

Table 3. Calibration curves slopes, linearities and detection limits for gaseous hydroxyl compounds and organic acids trapped on MTBSTFA coated Tenax TA tubes with post-sampling derivatisation process.

Standard Compound	Extracted ion	Calibration curve	Linearity	Detection limits		
	(m/z)	slope	(R^2)	ng tube^{-1}	ng m^{-3*}	ppt*
Alcohols						
5-Hydroxy-2-Pentanone	75	$(7 \pm 2) \times 10^4$	0.9769	0.5	42	10
HydroxyCyclohexanone	171	$(1.7 \pm 0.4) \times 10^3$	0.9576	5	417	89
Tert-Butyl-4-Hydroxy Butyrate	161	$(9 \pm 2) \times 10^4$	0.9830	0.2	17	2.6
(S)-3-Butene-1,2-diol	259	$(9 \pm 2) \times 10^2$	0.9578	10	834	232
1-Nonanol	201	$(1.1 \pm 0.3) \times 10^5$	0.9632	0.08	7	1.2
Farnesol	279	$(3.7 \pm 0.6) \times 10^3$	0.9840	3	250	28
Carboxylic acids						
Valeric acid	75	$(2.77 \pm 0.08) \times 10^5$	0.9989	0.09	8	1.9
Levulinic acid	75	$(1.8 \pm 0.1) \times 10^5$	0.9977	0.08	7	1.5
Heptanoic acid	75	$(1.83 \pm 0.05) \times 10^5$	0.9983	0.05	5	0.9
Mono-Methyl Fumarate	187	$(3.6 \pm 0.3) \times 10^5$	0.9941	0.07	6	1.1
6-OxoHeptanoic acid	117	$(2.3 \pm 0.2) \times 10^5$	0.9926	0.8	67	11
2,2-Dimethyl-3-HydroxyPropionic acid	147	$(1.2 \pm 0.2) \times 10^5$	0.9811	0.5	42	8.7
Succinic acid	289	$(3.4 \pm 0.2) \times 10^5$	0.9956	0.07	6	1.2
cis-Pinonic acid	171	$(3.2 \pm 0.3) \times 10^5$	0.9941	0.2	17	2.3
Perillic acid	223	$(3.9 \pm 0.3) \times 10^5$	0.9947	0.09	8	1.2
8-HydroxyOctanoic acid	331	$(5.6 \pm 0.7) \times 10^4$	0.9861	0.2	17	2.6
D-Malic acid	419	$(1.1 \pm 0.1) \times 10^5$	0.9872	0.8	67	12
Pinic acid	171	$(2.7 \pm 0.2) \times 10^5$	0.9913	0.3	25	3.3
4-OxoHeptanedioic acid	345	$(1.9 \pm 0.3) \times 10^5$	0.9746	2	167	23
3-CarboxyHexanedioic Acid	475	$(5 \pm 2) \times 10^4$	0.9368	2	167	21

* Given for a sampling volume of 2 m^3.

AMTD
5, 1153–1231, 2012

Table 4. Calibration curves slopes, linearities and detection limits for particulate hydroxyl compounds and organic acids trapped on Teflon-quartz fibres filters and MTBSTFA derivatised.

Standard Compound	Extracted ion (m/z)	Calibration curve slope	Linearity (R^2)	Detection limits ng filtre^{-1}	Detection limits ng m^{-3*}
Alcohols					
5-Hydroxy-2-Pentanone	75	$(1.0 \pm 0.2) \times 10^5$	0.9837	0.8	0.4
HydroxyCyclohexanone	171	$(1.8 \pm 0.3) \times 10^4$	0.9791	0.4	0.2
Tert Butyl-4-Hydroxy Butyrate	161	$(2.21 \pm 0.08) \times 10^5$	0.9988	0.04	0.02
(S)-3-Butene-1,2-diol	259	$(8.5 \pm 0.4) \times 10^4$	0.9967	0.04	0.02
1-Nonanol[a]	201	$(2.9 \pm 0.5) \times 10^5$	0.9633	0.04	0.02
Farnesol	279	$(3.6 \pm 0.2) \times 10^4$	0.9979	0.4	0.2
Carboxylic acids					
Valeric acid	75	$(8.6 \pm 0.3) \times 10^4$	0.9990	0.7	0.4
Levulinic acid[b]	75	$(1.2 \pm 0.4) \times 10^5$	0.9433	0.9	0.5
Heptanoic acid	75	$(1.5 \pm 0.2) \times 10^5$	0.9582	1.0	0.5
Mono-Methyl Fumarate	187	$(3.52 \pm 0.05) \times 10^5$	0.9999	0.2	0.1
6-OxoHeptanoic acid	117	$(2.15 \pm 0.08) \times 10^5$	0.9990	0.3	0.2
2,2-Dimethyl-3-HydroxyPropionic acid	147	$(3.5 \pm 0.2) \times 10^5$	0.9966	0.2	0.1
Succinic acid	289	$(5 \pm 2) \times 10^5$	0,8861	0.02	0.01
cis-Pinonic acid	171	$(3.4 \pm 0.5) \times 10^5$	0.9863	0.2	0.1
Perillic acid	223	$(4.32 \pm 0.05) \times 10^5$	0.9999	0.04	0.02
8-HydroxyOctanoic acid	331	$(2.33 \pm 0.07) \times 10^5$	0.9970	0.07	0.04
D-Malic acid	419	$(1.2 \pm 0.3) \times 10^5$	0.9623	0.07	0.04
Pinic acid	171	$(2.6 \pm 0.4) \times 10^5$	0.9887	0.3	0.2

* Given for a sampling volume of 2 m^3.

[a] 5 points from 80 to 1280 ng.

[b] 4 points from 160 to 1280 ng.

AMTD
5, 1153–1231, 2012

Table 5. Characteristic fragmentation of PFBHA and MTBSTFA derivatives in 1 EI and CI modes.

PFBHA derivatives EI ions	Fragments (*m/z*)	MTBSTFA derivatives EI ions	Fragments (*m/z*)	CI ions	Fragments (*m/z*)
181	$[C_6F_5CH_2]^+$	73	$[Si(CH_3)_3]^+$	M + 1	$[M + H]^+$
M – 181	$[M - C_6F_5CH_2]^+$	75	$[HOSi(CH_3)_2]^+$	M + 29	$[M + C_2H_5]^+$
M – 197	$[M - C_6F_5CH_2O]^+$	M – 15	$[M - CH_3]^+$	M + 41	$[M + C_3H_5]^+$
		M – 57	$[M - C(CH_3)_3]^+$		
		M – 115	$[M - Si(CH_3)_2C(CH_3)_3]^+$		
		M – 131	$[M - OSi(CH_3)_2C(CH_3)_3]^+$		

AMTD
5, 1153–1231, 2012

Table 6. Identification proposals for observed carbonyl compounds, organic acids and hydroxyls compounds from limonene ozonolysis experiment. D.: derivatised. G: observed in the gas phase. P: observed in the particulate phase.

Compound ID	Mass fragments	Tentative assignment							Phase(s)
		MW d.	Function number	MW not d.	Name	Structure	Identification	Reference	
					Carbonyls compounds (PFBHA derivatives)				
P1	EI: 181 (100), M – 181 = 112, M = 293 CI: M + 1 = 294 M + 29 = 322, M + 41 = 334	293	1	98	5-hexene-2-one		Nist EI list	Unique to this study	G-P
P2	EI: 42, 95(100), M – 181 = 152, 181, M = 333 CI: 95, 181, M + 1 = 334, M + 29 = 362, M + 41 = 374	333	1	138	Keto-Limonene		Proposed from mass spectra	Forester et al. (2009) Jaoui et al. (2007)	G
P3	EI: 181(100), M – 197 = 265, M = 462 CI: M + 1 = 463, M + 29 = 491, M + 41 = 503	462	2	72	Methyl Glyoxal		Proposed from mass spectra	Forester et al. (2010)	G-P
P4	EI: 181(100), M – 197 = 279, M = 476 CI: M + 1 = 477, M + 29 = 505, M + 41 = 517	476	2	86	DiMethyl Glyoxal		Standard	Unique to this study	G-P
P5	EI: 181(100), 279, M – 197 = 293, M – 181 = 309, M = 490 CI: M + 1 = 491, M + 29 = 519, M + 41 = 531	490	2	100	4-OxoPentanal		Standard	Forester et al. (2010)	G-P
P6	EI: 181(100), 320, 558, M – 197 = 361, M – 181 = 377, CI: M + 1 = 559, M + 29 = 587, M + 41 = 599	558	2	168	Limononaldehyde		Proposed from mass spectra	Leungsakul et al. (2005b) Jaoui et al. (2007)	G-P
P7	EI: 181(100), 305, M – 197 = 516, M = 713 CI: <Id	713	3	128	DiOxoHexanal		Proposed from mass spectra	Unique to this study	P
P8	EI: 138, 181(100), 319 M – 197 = 530, M = 727 CI: M + 1 = 728	727	3	142	3,6-DiOxoHeptanal		Proposed from mass spectra	Leungsakul et al. (2005b)	P
P9	EI: 94, 181(100), 347, M – 197 = 558, M – 181 = 574, M = 755 CI: <Id	755	3	170	Keto-Limononaldehyde		Proposed from mass spectra	Leungsakul et al. (2005b) Jaoui et al. (2007)	P
					Hydroxyl and carboxyl compounds (MTBSTFA derivatives)				
M1	EI: 75, 99, 145, M – 15 = 215, M – 57 = 173(100) CI: <Id	230	1	116	Levulinic Acid		Standard	Jaoui et al. (2006)	G
M2	EI: 73, 116, 147, M – 57 = 289(100), M – 15 = 331 CI: <Id	346	2	118	Succinic Acid		Standard	Jaoui et al. (2006)	G-P

AMTD
5, 1153–1231, 2012

Table 7. Continued.

Compound ID	Mass fragments	Tentative assignment							Phase(s)
		MW d.	Function number	MW not d.	Name	Structure	Identification	Reference	
M3	EI: 73(100), 123, 147, M – 57 = 303, M – 15 = 345 CI: 115, 173, 229, M – 57 = 303, M – 15 = 345, M + 1 = 361, M + 29 = 389, M + 41 = 401	360	2	132	2-MethylButanedioic Acid		Nist EI list match 75 %	Unique to this study	G
M4	EI: 73, 129, 147 M – 57 = 303(100), M – 15 = 345 CI: 115, 165, 229, M – 57 = 303, M – 15 = 345, M + 1 = 361, M + 29 = 389, M + 41 = 401	360	2	132	Pentanedioic Acid		Proposed from mass spectra	Jaoui et al. (2006)	G-P
M5	EI: 73, 133, 147, 157(100), 185, 215, 289, M – 57 = 317, M – 15 = 359 CI: 215, M – 57 = 317, M – 15 = 359, M + 1 = 375, M + 29 = 403, M + 41 = 415	374	2	146	α-KetoGlutaric Acid		Standard	Unique to this study	P
M6	EI: 73, 111, 141 M – 57 = 317(100), M – 15 = 359 CI: 257, M – 57 = 317, M – 15 = 359, M + 1 = 375, M + 29 = 403, M + 41 = 415	374	2	146	Hexanedioic Acid		Nist EI list match 92 %	Jaoui et al. (2006)	G-P
M7	EI: 73, 75, 111, 185, 317, M – 57 = 345(100), M – 15 = 387 CI: <ld	402	2	174	KetoNorLimonic Acid		Proposed from mass spectra	Jaoui et al. (2006)	P
M8	EI: 73, 75, 111, 185, 317, M – 57 = 345(100), M – 15 = 387 CI: <ld	402	2	174	4-OxoHeptanedioic Acid		Standard	Unique to this study	P
M9	EI: 73, 75, 147, M – 115 = 299, M – 57 = 357(100), M – 15 = 399, M = 414 CI: <ld	414	2	186	Limonic acid		Proposed from mass spectra	Jaoui et al. (2006), Leungsakul et al. (2005b)	G-P
M10	EI: 73, 75, 147, 185, 331, M – 57 = 359(100), M – 15 = 401 CI: <ld	416	2	188	KetoLimonic Acid		Proposed from mass spectra	Jaoui et al. (2006)	P
M11	EI: 73(100), 75, 99, 147, 225, 255, M – 57 = 385, M – 15 = 427 CI: <ld	442	2	214	3-Acetyl-4-MethylHept-3-enedioic Acid		Proposed from mass spectra	Unique to this study	P
M12	EI: 73(100), 115, 147, 287, M – 57 = 419, M – 15 = 461 CI: <ld	476	3	134	2-HydroxyButanedioic Acid (Malic Acid)		Standard	Unique to this study	P

AMTD
5, 1153–1231, 2012

Table 7. Continued.

Compound ID	Mass fragments	Tentative assignment							Phase(s)
		MW d.	Function number	MW not d.	Name	Structure	Identification	Reference	
M13	EI: 73(100), 133, 147, 171, 245, 273, 331, M – 57 = 433, M – 15 = 475 CI: <Id	490	3	148	2-HydroxyPentanedioic Acid		Nist EI list match 98 %	Unique to this study	P
M14	EI: 73(100), 115, 133, 147, 171, 273, M – 57 = 447, M – 15 = 489 CI: <Id	504	3	162	3-HydroxyHexanedioic Acid		Proposed from mass spectra	Unique to this study	P
M15	EI: 73, 147, 301, M – 131 = 387, M – 57 = 461(100), M – 15 = 503 CI: <Id	518	3	176	3-CarboxyPentanedioic Acid		Proposed from mass spectra	Unique to this study	P
M16	EI: 73, 147, 269, 301, 385, M – 131 = 401, M – 57 = 475(100), M – 15 = 517 CI: <Id	532	3	190	3-CarboxyHexanedioic Acid		Standard	Unique to this study	P

AMTD
5, 1153–1231, 2012

Table 8. Quantification of observed carbonyl compounds, organic acids and hydroxyl compounds.

Compound ID	Compound	Calibration standard	Gas phase concentration ($ng\,m^{-3}$)	Particulate phase concentration ($ng\,m^{-3}$)
	Carbonyl compounds (PFBHA derivatives)			
P1	5-hexene-2-one	3-pentene-2-one	166 ± 4	10 ± 4
P2	Keto-Limonene	dihydrocarvone	1830 ± 40	<lod[a]
P3	Methyl Glyoxal	Methyl Glyoxal	2500 ± 600	70 ± 30
P4	DiMethyl Glyoxal	DiMethyl Glyoxal	2500 ± 200	6.3 ± 0.9
P5	4-OxoPentanal	4-OxoPentanal	1760 ± 60	51 ± 3
P6	Limononaldehyde	4-OxoPentanal	7800 ± 300	640 ± 30
	Hydroxyl compounds and organic acids (MTBSTFA derivatives)			
M1	Levulinic Acid	Levulinic Acid	990 ± 60	nd[b]
M2	Succinic Acid	Succinic Acid	18 ± 1	7 ± 3
M3	2-MethylButanedioic Acid	Succinic Acid	4.8 ± 0.3	nd[b]
M4	Pentanedioic Acid	Succinic Acid	13.9 ± 0.9	4 ± 1
M6	Hexanedioic Acid	Succinic Acid	29 ± 2	12 ± 5
M9	Limonic acid	Pinic acid	2.9 ± 0.3	70 ± 10
M12	Malic Acid	Malic acid	nd[b]	12 ± 3
M13	2-HydroxyPentanedioic Acid	Malic acid	nd[b]	6 ± 2
M14	3-HydroxyHexanedioic Acid	Malic acid	nd[b]	17 ± 5

[a] limit of detection, [b] not detected

AMTD
5, 1153–1231, 2012

Table 9. Experimental partitioning coefficient K_i ($m^3\,mug^{-1}$) compared with K_i values ($m^3\,\mu g^{-1}$) estimated from theoretical saturation vapour pressures ($P^o_{L,i}$) calculated from 3 group contribution methods at 298 K. K_i calculation assumes a temperature of 300 K, a mean MW_{om} of 142 $g\,mol^{-1}$ and an activity coefficient γ_i of 1.27.

Compound ID	Compound	Experimental K_i	Estimated K_i values MY[a]	NAN[b]	SIM[c]
		Carbonyl compounds (PFBHA derivatives)			
P1	5-hexene-2-one	$1.3 \times 10^{-3} \pm 67\,\%$	4.54×10^{-9}	9.14×10^{-9}	7.26×10^{-9}
P3	Methyl Glyoxal	$1.3 \times 10^{-3} \pm 84\,\%$	2.14×10^{-9}	8.77×10^{-10}	6.49×10^{-9}
P4	DiMethyl Glyoxal	$7.4 \times 10^{-5} \pm 47\,\%$	7.11×10^{-9}	3.48×10^{-9}	7.00×10^{-9}
P5	4-OxoPentanal	$6.5 \times 10^{-4} \pm 34\,\%$	1.67×10^{-8}	1.45×10^{-8}	4.53×10^{-8}
P6	Limononaldehyde	$1.9 \times 10^{-3} \pm 34\,\%$	4.54×10^{-6}	1.35×10^{-6}	7.50×10^{-6}
		Hydroxyl compounds and organic acids (MTBSTFA derivatives)			
M2	Succinic Acid	$3.2 \times 10^{-2} \pm 73\,\%$	5.16×10^{-4}	3.00×10^{-4}	1.04×10^{-3}
M4	Pentanedioic Acid	$7.8 \times 10^{-3} \pm 73\,\%$	1.90×10^{-3}	1.08×10^{-3}	2.76×10^{-3}
M6	Hexanedioic acid	$6.9 \times 10^{-3} \pm 73\,\%$	6.49×10^{-3}	3.38×10^{-3}	6.50×10^{-3}
M9	Limonic Acid	$5.1 \times 10^{-1} \pm 50\,\%$	2.56×10^{-1}	2.51×10^{-2}	1.54×10^{-1}

[a] MY: Myrdal and Yalkowsky (1997); [b] NAN: Nannoolal et al. (2008); [c] SIM: Pankow and Asher (2008).

AMTD
5, 1153–1231, 2012

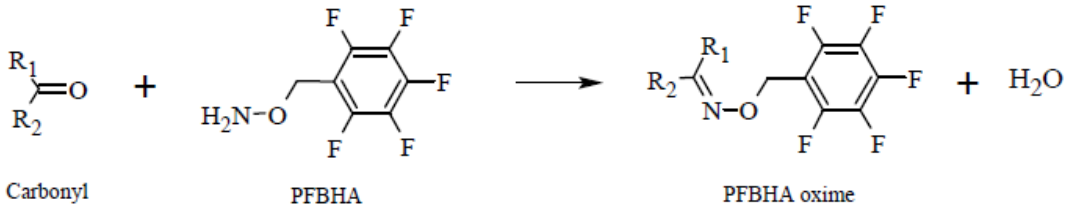

Fig. 1. Derivatisation reaction of carbonyl compound by PFBHA reagent.

AMTD
5, 1153–1231, 2012

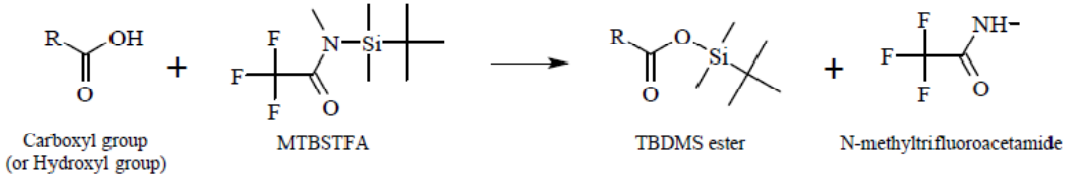

Fig. 2. Derivatisation reaction of carboxyl or hydroxyl compound by MTBSTFA reagent.

AMTD
5, 1153–1231, 2012

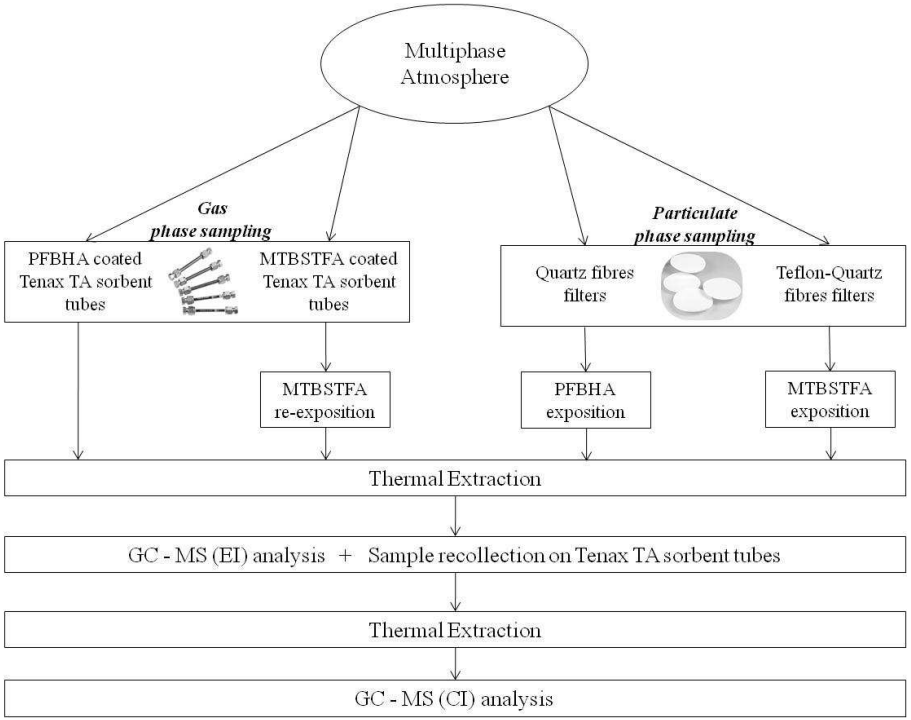

Fig. 3. Method overview.

AMTD
5, 1153–1231, 2012

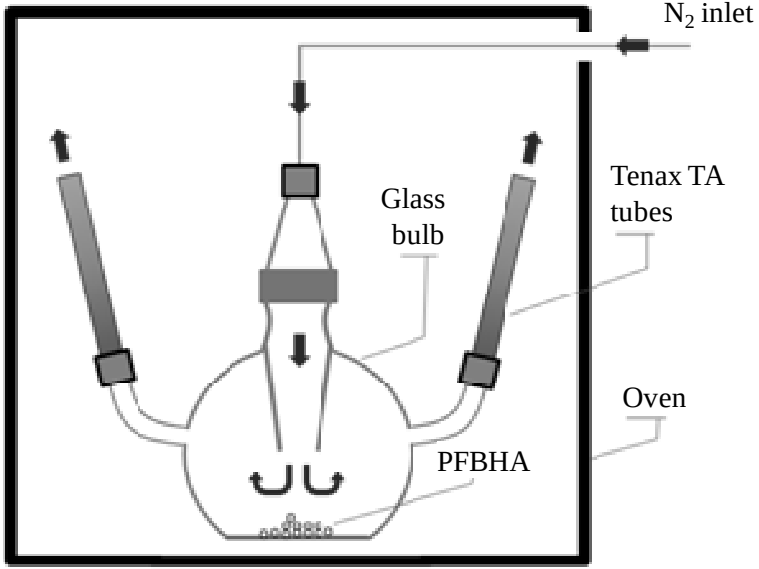

Fig. 4. Tenax TA tubes PFBHA coating process scheme.

AMTD
5, 1153–1231, 2012

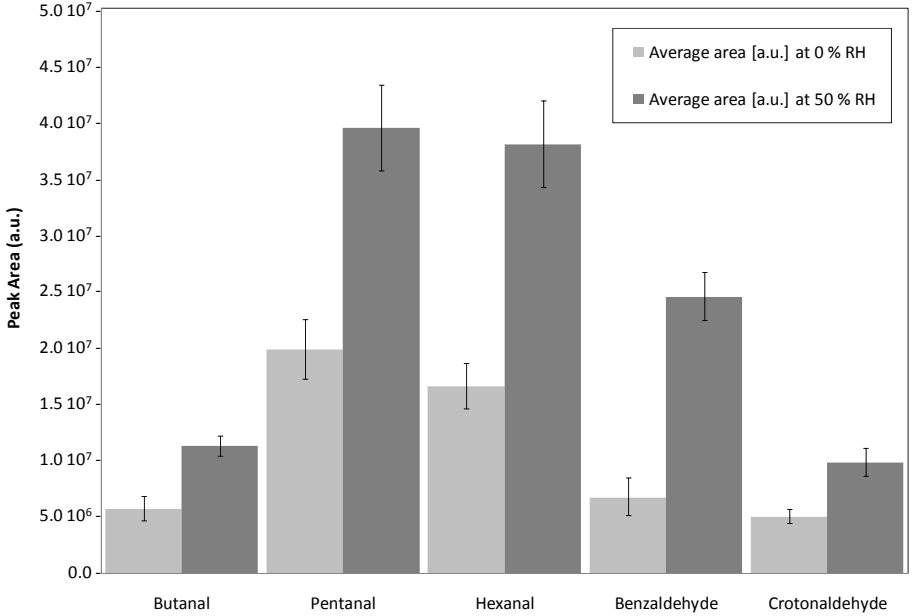

Fig. 5. Gaseous carbonyl compounds sampling on simulated atmosphere in dry (0 % RH) and wet (50 % RH) conditions. "Peak Area" refers to TIC EI chromatogram, in area unit. Error bars represent ±1 standard deviation determined from six replicates.

AMTD
5, 1153–1231, 2012

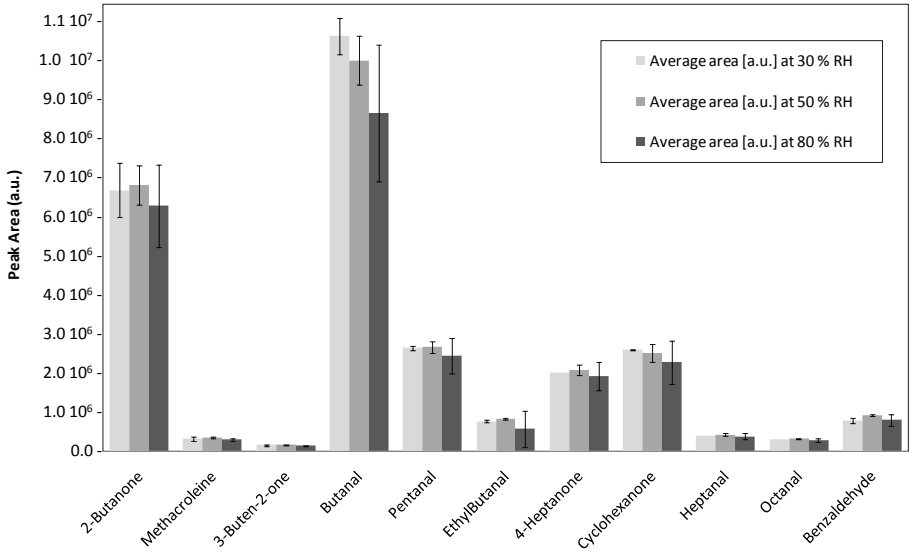

Fig. 6. Gaseous carbonyl compounds sampling on simulated atmosphere in realistic relative humidity range (30, 50 and 80 % RH). "Peak Area" refers to extracted ion EI chromatogram, in area unit (ion extraction depends on compound). Error bars represent ±1 standard deviation determined from three replicates.

AMTD
5, 1153–1231, 2012

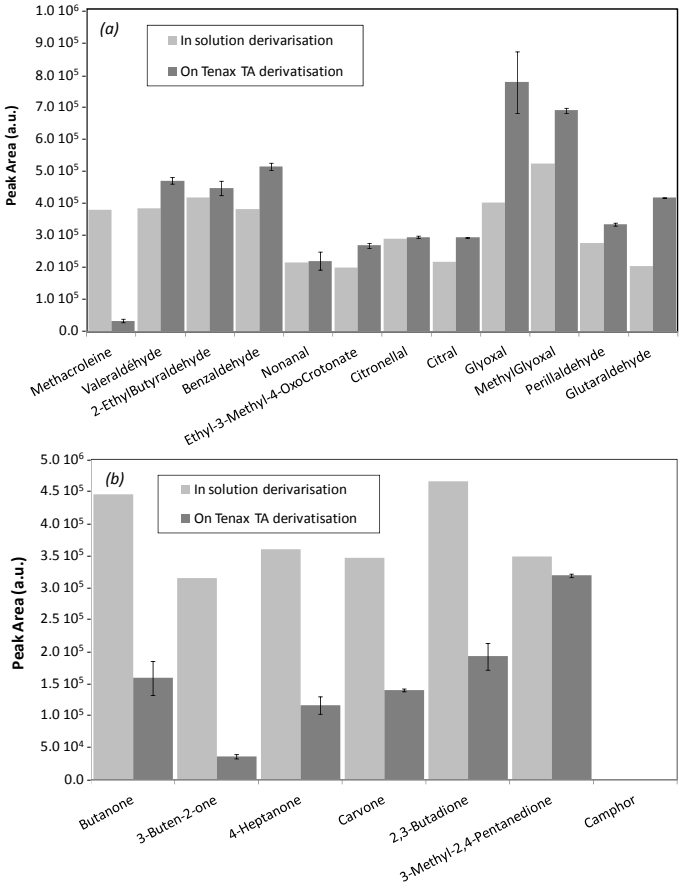

Fig. 7. In solution and on-Tenax TA carbonyl compounds PFBHA derivatisation results 2 comparison: **(a)** aldehydes derivatisation results, **(b)** ketones derivatisation results. "Peak Area" refers to FID chromatogram, in area unit. Error bars represent ±1 standard deviation determined from two replicates (no error bar for in solution derivatisation indicates only one replicate).

AMTD
5, 1153–1231, 2012

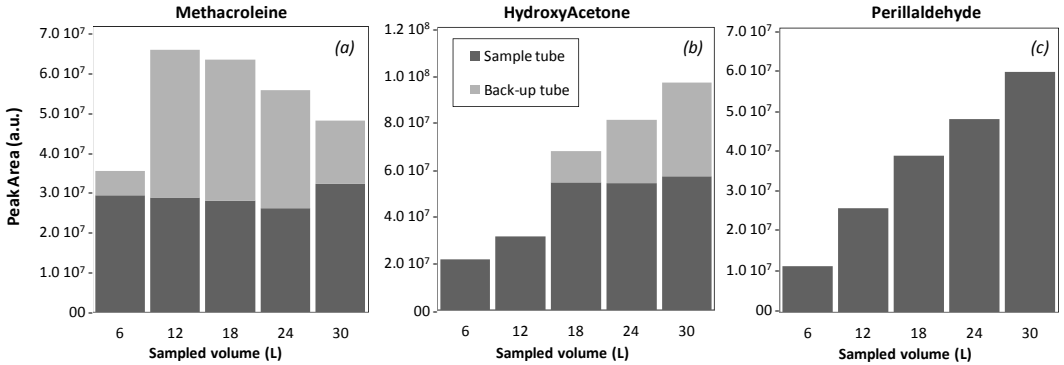

Fig. 8. Breakthrough volumes evaluation for carbonyl compounds on PFBHA coated Tenax TA sorbent tubes **(a)** Methacroleine, **(b)** HydroxyAcetone, **(c)** Perillaldehyde. "Peak Area" refers to *m/z* 181 extracted ion EI chromatogram, in area unit.

AMTD
5, 1153–1231, 2012

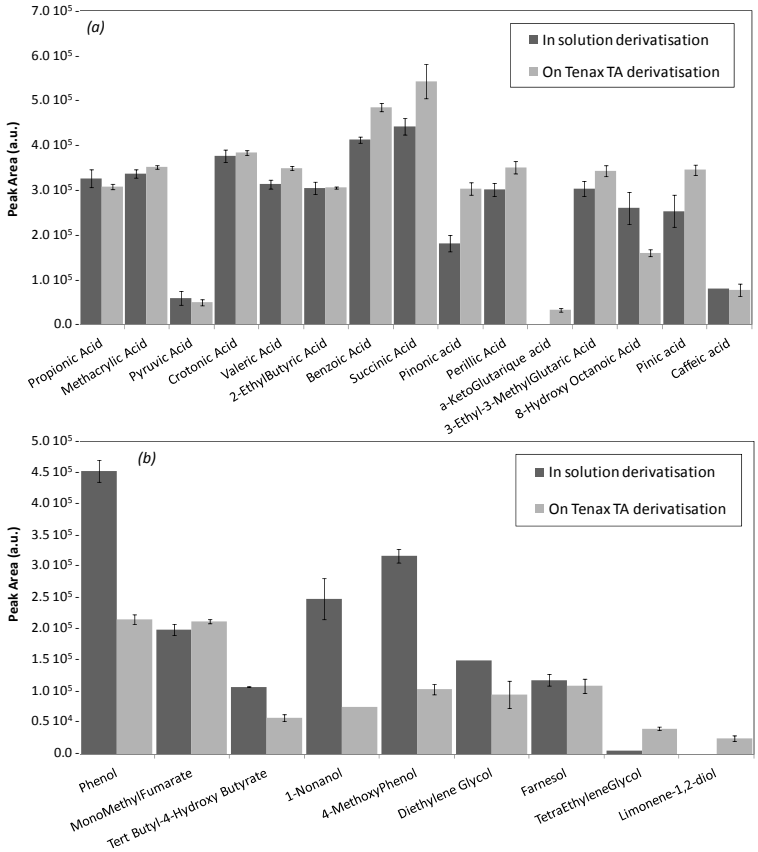

Fig. 9. In solution and on-Tenax TA carboxyl/hydroxyl compounds MTBSTFA derivatisation results comparison: **(a)** carboxylic acids derivatisation results, **(b)** hydroxylsderivatisation results. "Peak Area" refers to FID chromatogram, in area unit. Error bars represent ±1 standard deviation determined from three replicates for on-Tenax TA derivatisation and from two replicates for in solution derivatisation (no error bar indicates only one replicate).

AMTD
5, 1153–1231, 2012

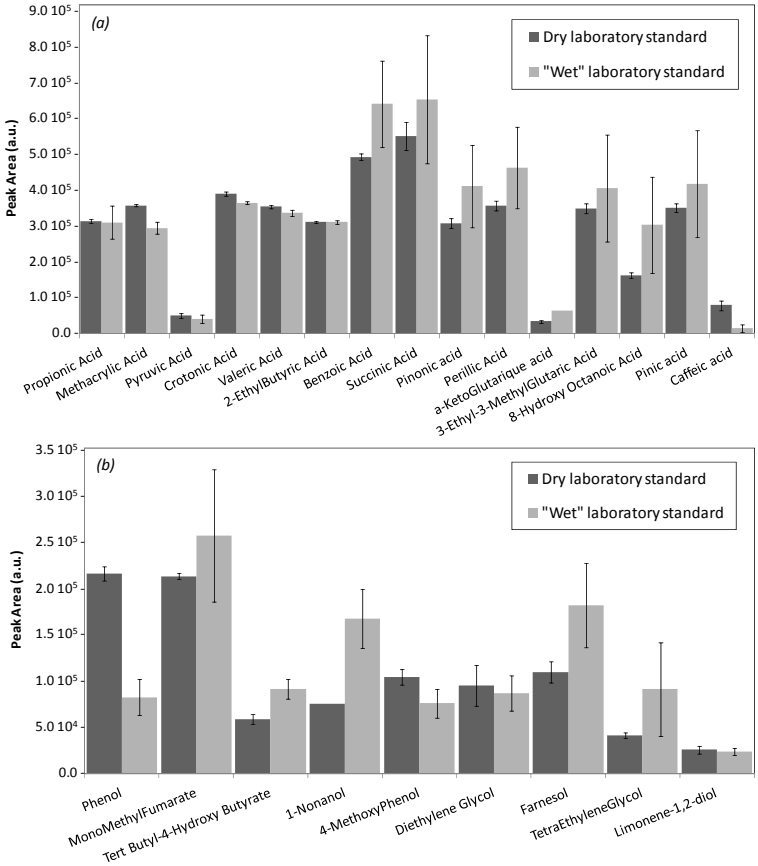

Fig. 10. Humidity influence on on-Tenax TA carboxyl/hydroxyl compounds MTBSTFA derivatisation: **(a)** carboxylic acids derivatisation results, **(b)** hydroxylderivatisation results. "Peak Area" refers to FID chromatogram, in area unit. Error bars represent ±1 standard deviation determined from three replicates.

AMTD
5, 1153–1231, 2012

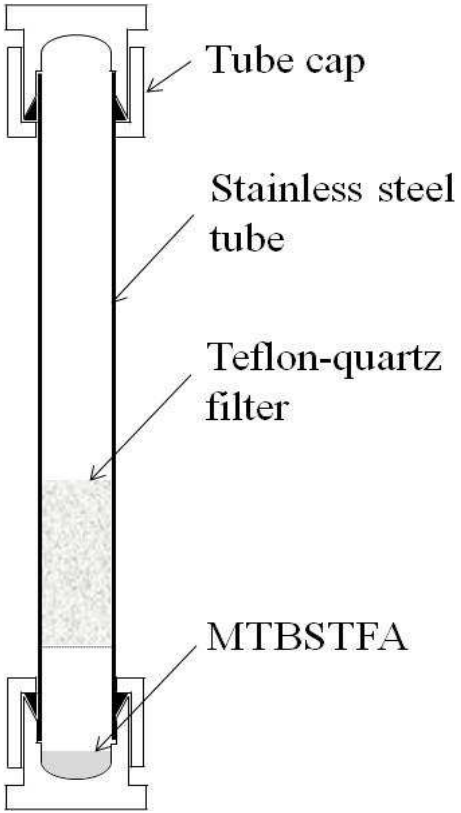

Fig. 11. Particulate phase MTBSTFA derivatisation scheme.

AMTD
5, 1153–1231, 2012

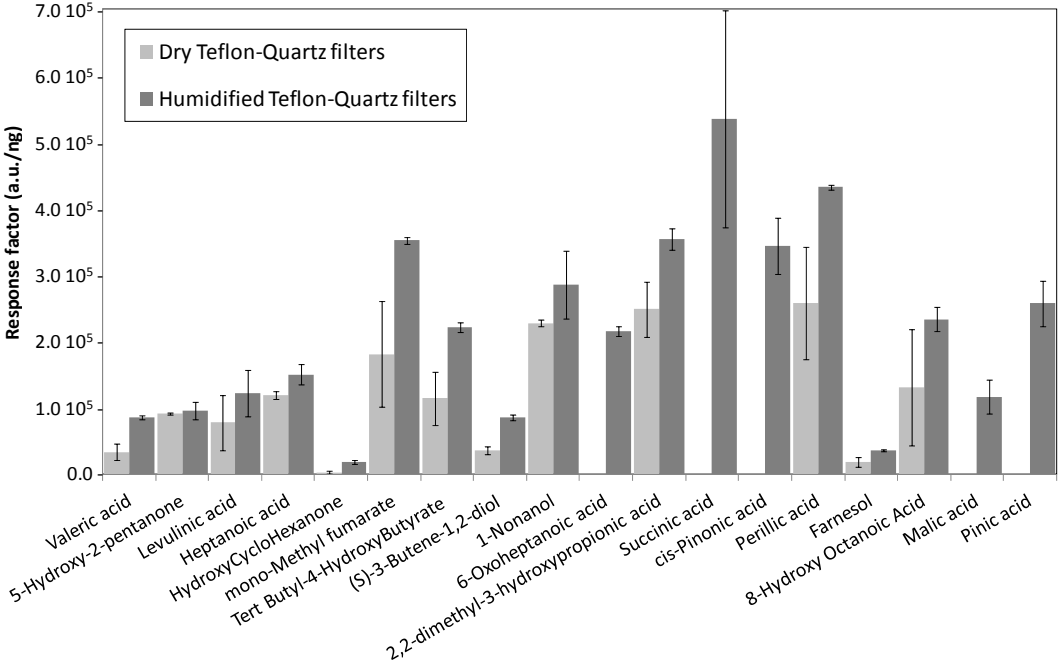

Fig. 12. Humidity influence on on-Teflon-quartz filters organic acids and hydroxyl compounds MTBSTFA derivatisation. Comparison is based on response factor evaluated from 5 points calibration curves (5 to 320 ng). "Response factor" refers to FID chromatogram surface peak area per ng of compound, in area unit. Error bars represent ±2 standard errors given for a 95 % confidence level.

AMTD
5, 1153–1231, 2012

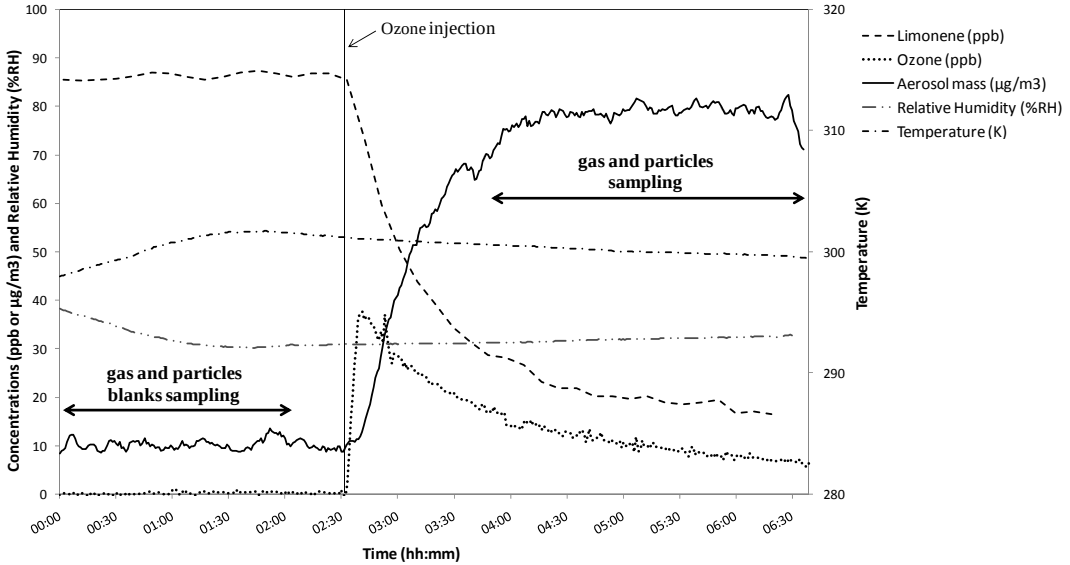

Fig. 13. Evolution of limonene ozonolysis experiment parameters.

AMTD
5, 1153–1231, 2012

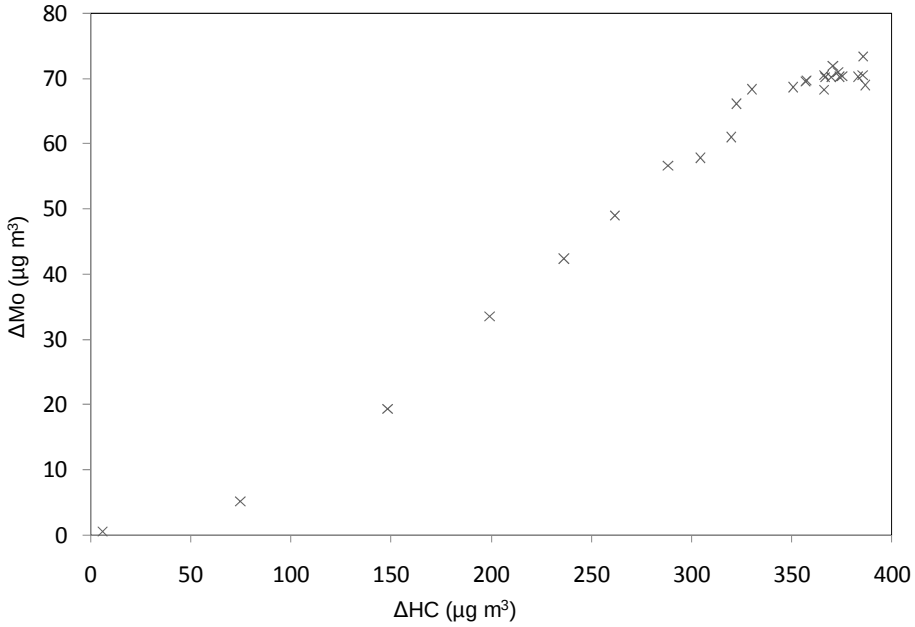

Fig. 14. Limonene ozonolysis experiment growth curve. Data corrected by dilution and wall losses.

AMTD
5, 1153–1231, 2012

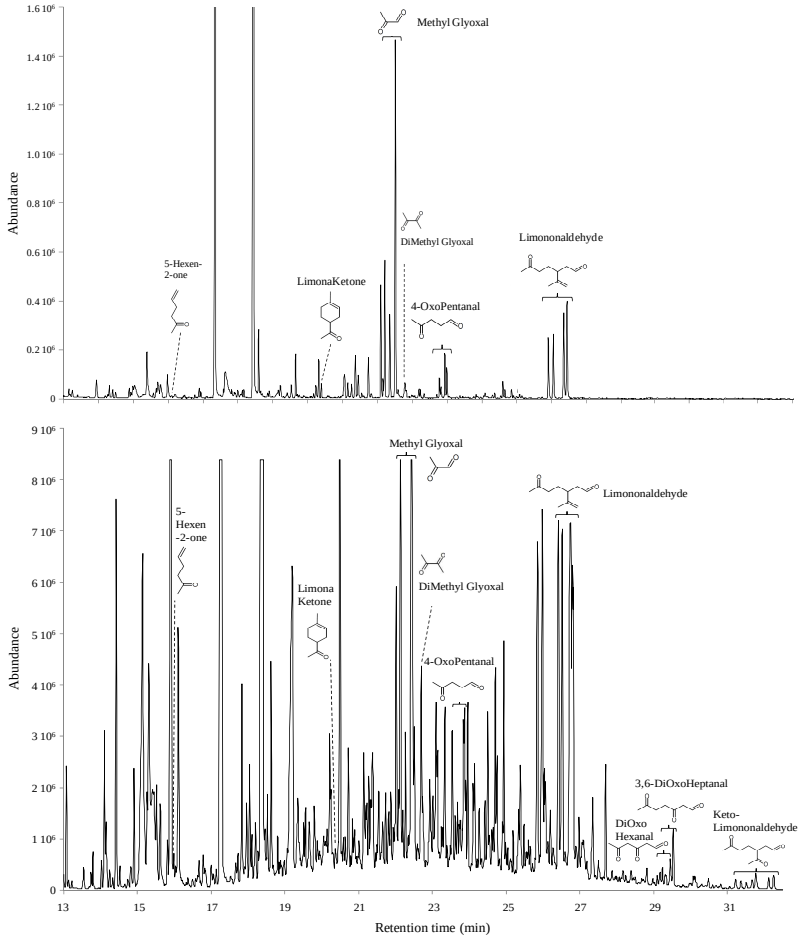

Fig. 15. Gas chromatograms of limonene ozonolysis products derivatised by PFBHA, EI selected ion *m/z* 181. Top chromatogram: gas phase. Bottom chromatogram: particulate phase.

AMTD
5, 1153–1231, 2012